Atmospheric Research

Leading patterns of the satellite-era summer precipitation over West Africa and associated global teleconnections

--Manuscript Draft--

Manuscript Number:	ATMOSRES-D-21-00325R2
Article Type:	Research Paper
Section/Category:	Climatology and climate change
Keywords:	Precipitation anomalies, Sahel, Guinea Coast, Sahel recovery, ITCZ, Walker Circulation
Corresponding Author:	Hyacinth Nnamchi University of Nigeria Nsukka, Nigeria
First Author:	Hyacinth Nnamchi
Order of Authors:	Hyacinth Nnamchi
	Victor Nnamdi Dike
	Akintomide A. Akinsanola
	Ugochukwu K. Okoro
Abstract:	Precipitation patterns over West Africa display a broad range of timescales, from the intraseasonal to decadal timescales, as well as multidecadal shifts. Here we investigate the dominant patterns of the July to September precipitation over the region and the related atmosphere-ocean anomalies during the satellite-era from 1983-2017. Using extended empirical orthogonal function analysis of an ensemble of nine precipitation datasets, we identify two dominant modes that together account for about 33% of the variance. The Sahel mode displays spatially coherent increases in precipitation over much of West Africa and a decrease at the Guinea Coast, and is closely reproduced by linear trend analysis. Linear trends explain 25-53% of the Sahel variance from the drier mid-1980s to the wetter mid-1990s. The Guinea Coast mode displays robust precipitation anomalies south of the Sahel, with strong interannual variability and a statistically non-significant trend. The Sahel mode is associated with a northerly displacement of the Inter-Tropical Convergence Zone (ITCZ), warm North Atlantic with cold blob in the subpolar gyre region, warm Mediterranean Sea, warm tropical southwest Indian Ocean and negative Pacific decadal variability pattern. The Atlantic Niño leads the Guinea Coast mode by two months. Both Sahel and Guinea Coast modes are substantially influenced by the interactions between meridional (displacements of the ITCZ) and zonal (variations of the Walker Circulation) atmospheric circulations. The southerly displacement of the ITCZ, convection, upper-level divergence and surface convergence in the equatorial Atlantic associated with the Guinea Coast mode is horizontally compensated by strong surface divergence and upper-level convergence over the equatorial Pacific where anomalous cooling prevails, implying a strong role for the Walker Circulation during this period. p {margin-bottom: 0.1in; line-height: 115%; background: transparent }
Suggested Reviewers:	
Response to Reviewers:	

Reviewer #1: The authors have diligently and exhaustively responded to my comments and suggestions. The paper is improved in clarity of content and delivery. I recommend acceptance (do not need to see the minor revisions recommended).

I only have one suggestion and a couple minor corrections to make:

The suggestion -- At the beginning of Section 2.3, can you please clarify how anomalies are computed? Is the mean that is subtracted that of each individual dataset (ensemble member), or that of the overall ensemble mean?

Minor editorial corrections --

p.9, ll.17-18: should read "we regress the precipitation anomalies on the normalized PCs and test for statistical significance using a two-tailed t-test." -- "we regress... and we test..."

p.10, l.18: should read "and dry years, that is, years ..." -- as is written, the second sentence does not stand on its own.

p.12, ll.11-12: should read "shows a monotonic increase in the JAS precipitation over the Sahel, but a decrease over parts of the Guinea Coast" -- a decrease... but an increase...

p.16, ll.4-6: should read "The link between summer precipitation over West Africa and global SST anomalies undergoes decadal variations (Giannini et al., 2003; Rodríguez-Fonseca et al., 2015). For instance, our analysis on the Sahel recovery period shows -- "the link undergoes...", "our analysis on the Sahel recovery..."

Reviewer #2: The revised manuscript is better than previous one. However, it still requires some modification before it can be published in AR.

1. The descriptions on the links between the SST anomalies (shown in Fig. 8) and atmospheric circulation anomalies (shown in Figs. 11-12) are lacking. E.g.,
Line 21 in page 16: "… is consistent with warm SST anomalies over North Atlantic".
Line 5 and 8 in page 17: "… is consistent with the Atlantic Nino pattern", "consistent with the anomalous equatorial Atlantic warming".
Line 7 in page 18: "can be linked to the cold SST anomalies there".
The authors draw these conclusions based on conjectures and/or references. In fact, the descriptions on SST anomalies above can be directly seen in Fig. 8. However, Fig. 8 is not referred to at all in section 4.2.

2. The authors may need to compact and improve the abstract.
(1) Too many results are presented, some seems to be unimportant information to readers. E.g., "The oceanic impacts are amplified by trends, particularly for the Sahel mode". Besides, "ocean impacts" here may be ambiguous to readers.
(2) The variance that each EOF mode accounts for may need be stated.
(3) The related SST anomalies for Sahel mode are clearly described (Line 11-13), but not for Guinea Coast mode. Why?
(4) The related atmospheric circulation anomalies for Guinea Coast mode (which accounts for 12.75% of the variance) are particularly highlighted with a five-line description (Line 17-21), but not for Sahel mode (which accounts for 20.56% of the variance). Why?

3. Keywords the authors listed may be not the best. The most important keyword "precipitation" is

not listed. "Inter-Tropical Convergence Zone (ITCZ)", which is as important as Walker Circulation in this paper, is also not listed. However, "Sahel" are listed twice. "Pacific teleconnections" has not been seen in the text, I suggest the authors to replace "Pacific teleconnections" by "teleconnection".

Responses to the specific comments and suggestions from Reviewer #1:

We very much appreciate your constructive and helpful comments. Your comments were invaluable in revising and improving our manuscript.

Our response to each comment is written in blue italic. The changes made have been ***tracked*** in the present version of the manuscript.

Reviewer #1: The authors have diligently and exhaustively responded to my comments and suggestions. The paper is improved in clarity of content and delivery. I recommend acceptance (do not need to see the minor revisions recommended).
I only have one suggestion and a couple minor corrections to make:

We have now addressed your comments and suggestions. Below are our specific responses.

The suggestion -- At the beginning of Section 2.3, can you please clarify how anomalies are computed? Is the mean that is subtracted that of each individual dataset (ensemble member), or that of the overall ensemble mean?
Suggestion accepted. It is now stated that for each ensemble member, the 1983-2017 time-mean at every grid-point was removed from the precipitation values for all years to create anomaly time series. ***(pages 8/9, lines 22-23/1)****.*

Minor editorial corrections --

p.9, ll.17-18: should read "we regress the precipitation anomalies on the normalized PCs and test for statistical significance using a two-tailed t-test." -- "we regress... and we test..."
Suggestion accepted. ***(page 9, lines 17-18).***

p.10, l.18: should read "and dry years, that is, years ..." -- as is written, the second sentence does not stand on its own.
Suggestion accepted. The two sentences have now been merged. ***(page 10, lines 17-19).***

p.12, ll.11-12: should read "shows a monotonic increase in the JAS precipitation over the Sahel, but a decrease over parts of the Guinea Coast" -- a decrease... but an increase...
Suggestion accepted. ***(page 12, lines 11-12).***

p.16, ll.4-6: should read "The link between summer precipitation over West Africa and global SST anomalies undergoes decadal variations (Giannini et al., 2003; Rodríguez-Fonseca et al., 2015). For instance, our analysis on the Sahel recovery period shows -- "the link undergoes...", "our analysis on the Sahel recovery..."
Suggestion accepted. ***(page 16, lines 4-6).***

Responses to the specific comments and suggestions from Reviewer #2:

We very much appreciate your constructive and helpful comments. Your comments were invaluable in revising and improving our manuscript.

Our response to each comment is written in blue italic. The changes made have been ***tracked*** in the present version of the manuscript.

Reviewer #2: The revised manuscript is better than previous one. However, it still requires some modification before it can be published in AR.

We have now revised the manuscript based on your comments and suggestions. Please find our specific responses below.

1. The descriptions on the links between the SST anomalies (shown in Fig. 8) and atmospheric circulation anomalies (shown in Figs. 11-12) are lacking. E.g.,
Line 21 in page 16: "… is consistent with warm SST anomalies over North Atlantic".
Line 5 and 8 in page 17: "… is consistent with the Atlantic Nino pattern", "consistent with the anomalous equatorial Atlantic warming".
Line 7 in page 18: "can be linked to the cold SST anomalies there".
The authors draw these conclusions based on conjectures and/or references. In fact, the descriptions on SST anomalies above can be directly seen in Fig. 8. However, Fig. 8 is not referred to at all in section 4.2.
Suggestion accepted. Fig. 8 is now referred to to link the SST anomalies and atmospheric circulation anomalies.
(page 16, line 22).
(page 17, line 5).
(page 17, line 8).
(page 18, line 7).

2. The authors may need to compact and improve the abstract.
We have now revised the Abstract. The specific changes made are stated below.

(1) Too many results are presented, some seems to be unimportant information to readers. E.g., "The oceanic impacts are amplified by trends, particularly for the Sahel mode". Besides, "ocean impacts" here may be ambiguous to readers.
Suggestion accepted. The sentence referred to has now been removed. ***(page 2, line 15)****.*

(2) The variance that each EOF mode accounts for may need be stated.
The total variance explained by the two leading EOFs of interest is stated in the Abstract. ***(page 2, lines 5-7)****.*

However stating variances explained of the individual EOFs here will lead to ***having percentages (%) four times in the Abstract****. We feel that this will hamper clarify.*

(3) The related SST anomalies for Sahel mode are clearly described (Line 11-13), but not for Guinea Coast mode. Why?

Please note that strongest SST anomalies associated with the Guinea Coast mode occur in the equatorial Pacific and equatorial Atlantic as shown in Fig. 10. We discussed the connection between SST anomalies in these regions and atmospheric anomalies using this sentence. ***(page 2, lines 18-22).***

"The ***Atlantic Niño leads*** the ***Guinea Coast mode*** by two months… The southerly displacement of the ITCZ, convection, upper-level divergence and surface convergence in the ***equatorial Atlantic*** associated with the ***Guinea Coast mode*** is horizontally compensated by strong surface divergence and upper-level convergence over the ***equatorial Pacific*** where ***anomalous cooling*** prevails, implying a strong role for the Walker Circulation during this period."

(4) The related atmospheric circulation anomalies for Guinea Coast mode (which accounts for 12.75% of the variance) are particularly highlighted with a five-line description (Line 17-21), but not for Sahel mode (which accounts for 20.56% of the variance). Why?
In this revision, we have now stated that the Sahel mode is associated with a northerly displacement of the Inter-Tropical Convergence Zone (ITCZ). ***(page 2, lines 11-12)****.*

We particularly try to provide a context for the time-lag between the Atlantic Niño and Guinea Coast mode.

3. Keywords the authors listed may be not the best. The most important keyword "precipitation" is not listed. "Inter-Tropical Convergence Zone (ITCZ)", which is as important as Walker Circulation in this paper, is also not listed. However, "Sahel" are listed twice. "Pacific teleconnections" has not been seen in the text, I suggest the authors to replace "Pacific teleconnections" by "teleconnection".
Suggestions partly accepted. We have now listed "precipitation anomalies" and "ITCZ" listed as a keyword and Pacific teleconnections removed. ***(page 2, lines 22-23).***

We however retain"Sahel" and "Sahel recovery" as keywords. We note that Sahel (the transition zone between humid/coastal West Africa and the Sahara desert) and Sahel recovery (the question of whether a phase shift from the prolonged drought in that region during the 1970s/1980s has occurred) are distinct keywords in our manuscript.

Leading patterns of the satellite-era summer precipitation over West Africa and global associated teleconnections

Hyacinth C. Nnamchi[a], Victor N. Dike[b,c] and Akintomide A. Akinsanola[d] and Ugochukwu K. Okoro[e]

[a]GEOMAR Helmholtz Centre for Ocean Research Kiel, Düsternbrooker Weg 20, 24105 Kiel, Germany

[b]International Center for Climate and Environment Sciences, Institute of Atmospheric Physics, Chinese Academy of Sciences, Beijing 100029, China

[c]Energy, Climate, and Environment Science Group, Imo State Polytechnic Umuagwo, Ohaji, PMB 1472 Owerri, Imo State, Nigeria

[d]Department of Geography, University of Georgia, Athens, Georgia, United States of America

[e]Atmospheric Physics Group, Department of Physics, Imo State University, Owerri, Nigeria

Highlights

-Sahel and Guinea Coast precipitation modes identified by extended EOF analysis

-Trends explain 25-53%% of the Sahel variance from 1983-1995 to 2017

-Impacts of SST anomalies on both modes amplified by linear trends

-Atlantic Niño leads the Guinea Coast mode by two months

-Interaction of meridional and zonal atmospheric circulations important for both modes

Leading patterns of the satellite-era summer precipitation over West Africa and global associated teleconnections

Hyacinth C. Nnamchi[a], Victor N. Dike[b,c] and Akintomide A. Akinsanola[d] and Ugochukwu K. Okoro[e]

[a]GEOMAR Helmholtz Centre for Ocean Research Kiel, Düsternbrooker Weg 20, 24105 Kiel, Germany

[b]International Center for Climate and Environment Sciences, Institute of Atmospheric Physics, Chinese Academy of Sciences, Beijing 100029, China

[c]Energy, Climate, and Environment Science Group, Imo State Polytechnic Umuagwo, Ohaji, PMB 1472 Owerri, Imo State, Nigeria

[d]Department of Geography, University of Georgia, Athens, Georgia, United States of America

[e]Atmospheric Physics Group, Department of Physics, Imo State University, Owerri, Nigeria

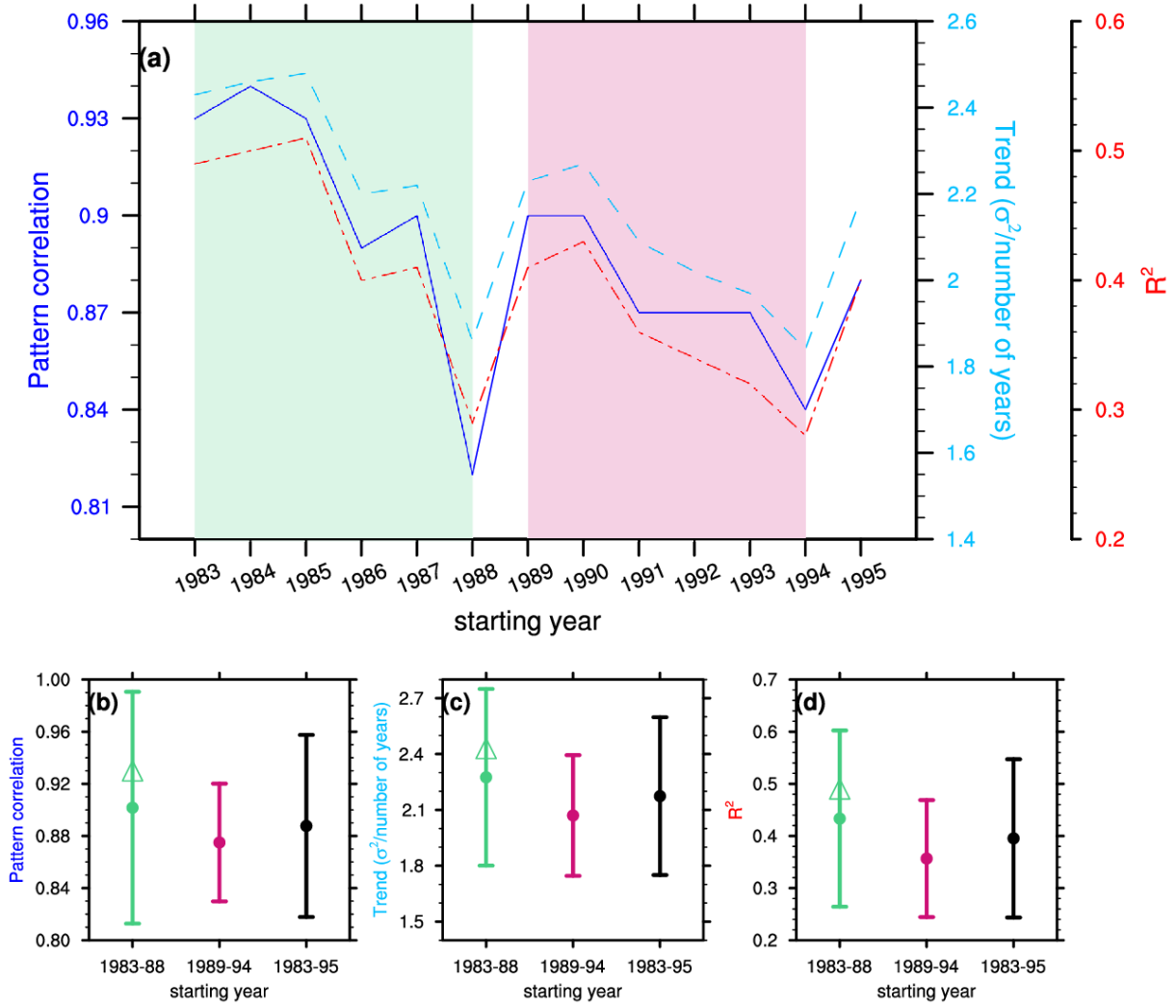

Sensitivity of the Sahel pattern to the choice of starting years from 1983-1995 to 2017

Leading patterns of the satellite-era summer precipitation over West Africa and global associated teleconnections

Hyacinth C. Nnamchi[a], Victor N. Dike[b,c] and Akintomide A. Akinsanola[d] and Ugochukwu K. Okoro[e]

[a]GEOMAR Helmholtz Centre for Ocean Research Kiel, Düsternbrooker Weg 20, 24105 Kiel, Germany

[b]International Center for Climate and Environment Sciences, Institute of Atmospheric Physics, Chinese Academy of Sciences, Beijing 100029, China

[c]Energy, Climate, and Environment Science Group, Imo State Polytechnic Umuagwo, Ohaji, PMB 1472 Owerri, Imo State, Nigeria

[d]Department of Geography, University of Georgia, Athens, Georgia, United States of America

[e]Atmospheric Physics Group, Department of Physics, Imo State University, Owerri, Nigeria

Highlights

-Sahel and Guinea Coast precipitation modes identified by extended EOF analysis

-Trends explain 25-53%% of the Sahel variance from 1983-1995 to 2017

-Impacts of SST anomalies on both modes amplified by linear trends

-Atlantic Niño leads the Guinea Coast mode by two months

-Interaction of meridional and zonal atmospheric circulations important for both modes

Abstract

Precipitation patterns over West Africa display a broad range of timescales, from the intraseasonal to decadal timescales, as well as multidecadal shifts. Here we investigate the dominant patterns of the July to September precipitation over the region and the related atmosphere-ocean anomalies during the satellite-era from 1983-2017. Using extended empirical orthogonal function analysis of an ensemble of nine precipitation datasets, we identify two dominant modes that together account for about 33% of the variance. The Sahel mode displays spatially coherent increases in precipitation over much of West Africa and a decrease at the Guinea Coast, and is closely reproduced by linear trend analysis. Linear trends explain 25-53% of the Sahel variance from the drier mid-1980s to the wetter mid-1990s. The Guinea Coast mode displays robust precipitation anomalies south of the Sahel, with strong interannual variability and a statistically non-significant trend. The Sahel mode is associated with ~~linked to~~ a northerly displacement of the Inter-Tropical Convergence Zone (ITCZ), warm North Atlantic with cold blob in the subpolar gyre region, warm Mediterranean Sea, warm tropical southwest Indian Ocean and negative Pacific decadal variability pattern. The Atlantic Niño leads the Guinea Coast mode by two months. ~~The oceanic impacts are amplified by trends, particularly for the Sahel mode.~~ Both Sahel and Guinea Coast modes are substantially influenced by the interactions between meridional (displacements of the ~~Inter-Tropical Convergence Zone,~~ ITCZ) and zonal (variations of the Walker Circulation) atmospheric circulations. The southerly displacement of the ITCZ, convection, upper-level divergence and surface convergence in the equatorial Atlantic associated with the Guinea Coast mode is horizontally compensated by strong surface divergence and upper-level convergence over the equatorial Pacific where anomalous cooling prevails, implying a strong role for the Walker Circulation during this period.

Keywords: Precipitation anomalies, Sahel, Guinea Coast, Sahel recovery, ITCZ, Walker Circulation~~, Guinea Coast,ITCZ Pacific teleconnections~~

1. Introduction

Precipitation is of great importance to the environment and socio-economic activities in West Africa, and its variability and change have significant impacts on agriculture, water resources, hydroelectricity generation, and industrial production (Sobral et al., 2020; Washington et al., 2006). During the instrumental era, the region has experienced strong fluctuations, with pronounced variability across a wide range of temporal scales, from intraseasonal to interannual and decadal time scales (Balas et al., 2007; Le Barbé et al., 2002; Maloney and Shaman, 2008; Mohino et al., 2011; Nash et al., 2016; Nicholson, 2008; Nicholson et al., 2018; Sultan et al., 2005, 2003; Sylla et al., 2016, 2010; Washington et al., 2006).

Two distinct precipitation zones are generally recognized over West Africa, namely the Guinea Coast to the south and the Sahel to the north, with transition around 10°N (Nguyen et al., 2011; Nicholson and Grist, 2001; Nicholson and Webster, 2007; Nnamchi and Li, 2011; Worou et al., 2020). On interannual and decadal timescales, distinct patterns of tropical Atlantic sea surface temperature (SST) anomalies have been linked to the Guinea Coast and Sahel precipitation, respectively. Increased precipitation at the Guinea Coast is associated with Atlantic Niño warm events (Giannini et al., 2003; Rodríguez-Fonseca et al., 2015; Wagner and Silva, 1994; Worou et al., 2020; Zhao-Hui and Dike, 2018), often linked to cold events in the South Atlantic extratropics (Nnamchi et al., 2011; 2013; Nnamchi and Li, 2016; Worou et al., 2020). The Atlantic Niño–related anomalous increases in precipitation over the Guinea Coast can occur concurrently with decreases over the Sahel (Nnamchi et al., 2011; Polo et al., 2008; Vallès-Casanova et al., 2020).

Although extreme precipitation events exhibit significantly increasing trends in parts of the Guinea Coast, the annual precipitation trends are not strong (Nkrumah et al., 2019; Sanogo et al., 2015). The weak trends in this region may reflect the impacts of interannual and decadal precipitation variability. Nicholson et al., (2018) shows that during the period 1883-2014, the annual precipitation averaged over the Guinea Coast exhibits a negative trend but this was not statistically significant.

However, the trend maps for May-September during 1980-2010 shows large variations across the region in different datasets (Sylla et al., 2016).

Precipitation changes and variability over the semi-arid Sahel are associated with distinct patterns of SST anomalies in the tropical Atlantic, Pacific, and Indian Oceans (Bader and Latif, 2003; Diatta and Fink, 2014; Giannini et al., 2003; 2019; Losada et al., 2012; Nicholson and Grist, 2001; Polo et al, 2008; Paeth et al., 2011).

While instrumental records have shown cycles of wet and dry conditions over the Sahel, it has been suggested that a change in precipitation regime from wetter conditions to drier conditions may have occurred over the Sahel during the late 1960s or early 1970s (Nicholson et al., 2018). Dry conditions tend to be more or less coherent over the Sahel, associated with a weakening in the pressure gradient between ocean and land, and thus, weaker inland moisture penetration (Lélé et al, 2015; Lélé and Leslie, 2016). Both observational and numerical modelling studies have suggested precipitation recovery over the Sahel since the late 1980s to the early 1990s (Druyan, 2011; Fontaine et al., 2011; Sylla et al., 2016; Lebel & Ali, 2009; Nicholson et al., 2018; Sanogo et al., 2015; Akinsanola and Zhou 2019). This implies that, in contrast to the widespread drying of the 1970s-1980s, the Sahel may have witnessed a partial recovery in precipitation during the subsequent years.

The precipitation recovery results from an increase in the number of wet days over the entire Sahel, as well as an increase in precipitation intensity in the central part of the Sahel during 1981-2014 (Bichet & Diedhiou, 2018). The increased Sahel precipitation has been linked to strong northward migration of deep convection since the mid-1990s (Fontaine et al., 2011;Lélé et al, 2015), partly resulting from the impact of North Atlantic SST anomalies that may have also been influenced by aerosols (Biasutti, M., 2019; Biasutti and Giannini, 2006; Giannini & Kaplan, 2019; Giannini et al., 2013; Mohino et al., 2011; Pomposi et al., 2020; Rostayn and Lohmann, 2002;). Furthermore, a warm Mediterranean Sea is associated with intense West African Monsoon, stronger low-level moisture

advection, and a northward location of ascending motions over the Sahel, causing increases in precipitation (Park et al., 2016; Worou et al., 2020).

However, there is a geographical variation to the pattern of the Sahel precipitation recovery. Precipitation over central Sahel increased by about 10% from 1990 through 2007 compared to 1970–1989, but was still lower than 1950-1969 mean, while in the western Sahel the precipitation deficit remained unchanged (Lebel & Ali, 2009). The increased precipitation in the central eastern Sahel during 1980-2012 was associated with increased vertical moisture advection (Akinsanola and Zhou, 2019). Century-long rain gauge time series over the region from 11-17°N suggests more robust precipitation recovery in the West African part of the Sahel than in the Horn of African part (Nicholson et al., 2018).

It must be stated that the reported changes in precipitation partly depend on the choice of the reference dataset which can cause discrepancies in the estimates of the precipitation recovery over West Africa (Atiah et al., 2020; Sylla et al., 2013). The number of rain gauge stations over Africa included in the different gridded datasets displays a systematic decline since the 1980s, which may partly reflect time lapse until the historical data are included in the archives (Becker et al., 2013). Specifically, the number of rain gauge stations included in the Global Precipitation Climatology Centre (GPCC) dataset (Schneider et al., 2020) decreased from 7372 in 1981-1985 to 957 during 2015-2019 (Fig. 1). The overall low density of gauge network coupled with this decline denotes a source of uncertainty in the region's precipitation (Hewitson et al., 2014; Schneider et al., 2017; Washington et al., 2006). Thus, there are marked differences among various datasets over the region during the recent decades (Akinsanola et al., 2016; Satge et al., 2020; Sylla et al., 2016). The implication is that the choice of datasets could, to a certain degree, introduce variations in the interpretation of causative mechanisms of the observed precipitation (Liu et al., 2019).

Interestingly, the period since the 1980s coincides with the satellite-era in global observations of the atmosphere and oceans. This represents improvements in observations, partly through the combination of rain-gauge measurements with satellite estimates of precipitation, and this is vital in regions with few rain-gauge measurements such as West Africa (Cavalcante et al., 2020; Schneider et al., 2017; Suliman et al., Washington et al., 2006; Yu et al., 2020).

Here we use an ensemble of nine datasets consisting of rain-gauge and satellite-derived products to investigate the dominant patterns of precipitation anomalies over West Africa (0°-20°N, 20°W-20°E) during the satellite-era 1983-2017. By using this ensemble, we aim to reduce the uncertainties in the precipitation observations (Liu et al., 2019) and focus on the robust patterns. We employ the extended empirical orthogonal functions (extended-EOF) analysis, which is based on a matrix of the nine-member observational ensemble. We investigate trends and interannual variability of the northern hemisphere summer precipitation, including sensitivity of the analysis to the choice of starting and ending dates, from the drier mid-1980s to the wetter mid-1990s. Although the rainy season is typically longer at the Guinea Coast, this study focuses on the July-August-September (JAS), when the maximum precipitation is received over the semi-arid Sahel (Dunning et al., 2016; Liebmann et al., 2012; Sultan and Janicot, 2003), and indeed the entire West Africa as seen in Fig. 2.

It is known that global SST anomalies, through their impacts on atmospheric circulation, are key to precipitation anomalies over West Africa (Giannini et al., 2003; Giannini and Kaplan, 2019; Giannini et al., 2013; Held et al., 2005; Pomposi et al., 2020; Steinig et al., 2018). The SST anomalies also mediate the externally-forced impacts of atmospheric aerosols and greenhouse gases (Bellomo et al., 2018; Biasutti and Giannini, 2006; Booth et al., 2012; Haustein et al., 2019; Nnamchi et al., 2020; Rostayn and Lohmann, 2002; Tokinaga and Xie, 2011). Thus, we investigate the distinct patterns of SST anomalies associated with the satellite-era precipitation in the region, as well as the related atmospheric circulation anomalies.

The paper is organized as follows. Section 2 describes the data and methodology, the leading precipitation patterns and related ocean-atmosphere teleconnections are presented in Sections 3 and 4, respectively. Section 5 provides summary and conclusions.

2. Data and Methodology

2.1 Data

We have assembled nine different precipitation datasets derived from rain-gauge measurements or a combination of rain-gauge and satellite measurements. Information on the datasets including the spatial resolution, reference, and types of measurement are summarized in Table 1. A common period in all datasets (1983-2017) form the basis for our analysis. The precipitation datasets were used to construct an ensemble, so that the individual datasets denote the ensemble members from which we calculated the ensemble-mean.

In addition, we analyzed satellite-derived SST on 1° × 1° longitude-latitude global grids (Reynolds et al., 2002), top-of-the-atmosphere outgoing longwave radiation (OLR) on 2.5° × 2.5° grids (Liebmann and Smith, 1996), as well as the European Centre for Medium-Range Weather Forecasts fifth generation atmospheric reanalysis on 0.25° × 0.25° grids and 37 pressure levels (Hersbach et al., 2020). The velocity potential and divergent winds were estimated from the reanalysis horizontal wind components via spherical harmonics.

2.2 Data intercomparison

Precipitation over West Africa exhibits seasonal characteristics associated with the monsoon system (Froidurot and Diedhiou, 2017). The nine gridded precipitation datasets analyzed realistically capture the seasonal evolution of precipitation, with the mean and standard deviation—representing the interannual variability—peaking in August (Fig. 2). Nonetheless, there are some notable spreads in the mean and standard deviation. With an ensemble-mean of 161.6 mm month^{-1}, the mean precipitation in

August ranges from 135.3 mm month^{-1} (ARC2) to 171.6 mm month^{-1} (CHIRPS). The interannual variability exhibits a strong spread with the multi-data standard deviation of 11.6 mm month^{-1} in August.

Previous studies discussed systematic differences between satellite estimates and products derived exclusively from rain gauges (Dunning et al., 2016; Novella and Thiaw, 2012). In our analysis, two satellite-derived datasets (ARC2 and CPC) underestimated while another two (CHIRPS and GPCP) overestimated the mean precipitation during the rainy months. Four datasets, consisting of two in-situ (GPCC and UDEL) and two satellite-derived (ARC2 and CPC) products overestimated the ensemble mean standard deviation. It is overall rather difficult to see an overall systematic difference between satellite estimates and exclusively rain gauge products averaged over West Africa in our nine-member ensemble.

The rest of this study focuses on the three-month season JAS during which the maximum precipitation is recorded. During this season, mean and standard deviations of precipitation decreases systematically with latitude, with the highest (lowest) values over Guinea coast (Sahel) in all datasets (Fig. 3). Furthermore, there are two localized regions of maximum precipitation associated with localised orography over the Fouta Djallon highlands and the Cameroon Mountains (Akinsanola et al., 2018), where precipitation amounts exceed 250 mm month^{-1}. However, the maxima in these regions appear to be underestimated in ARC2 and CPC (Fig. 2a and d, respectively) which also have comparatively low region-averaged precipitation (Fig. 2a). Both ARC2 and CPC are satellite products.

2.3 Statistical analysis

We construct an ensemble of the nine precipitation datasets over West Africa using JAS data. For each ensemble member, t~~T~~he 1983-2017 time-mean at every grid-point was removed from the precipitation

values for all years to create anomaly time series. We conceptualize the JAS precipitation anomaly time series at each grid-point $X(t, z, \mathbf{s})$ as consisting of two major components:

$$X(t,z,s) = X_{\Delta}(t,z,s) + X_{\sigma}(t,z,s).X_{noise} \quad (1)$$

where t is the time function varying from 1983 (t=1) to 2017 (t=35), z is the ensemble dimension containing the nine precipitation datasets, and the vector **s** represents longitude-latitude grid points, X_{Δ} is trend and X_{σ} is variability component. We consider the trend component as a least-squares linear fit to the data, so that the stochastic climate noise (X_{noise}) scales the variability component.

We applied extended-EOF analysis to the ensemble raw precipitation anomaly dataset (composed of both trend and interannual variability components) to determine the dominant patterns. Each extended-EOF mode (dimensioned z,**s**) consists of nine maps each representing the individual datasets, and is associated with a single principal component (PC) time series. The advantage of this approach is that it acts as a filter in the ensemble dimension, so that each PC captures the strongest signals in all nine precipitation datasets.

The first two extended-EOF modes together account for 33.3% of the summer precipitation variance over West Africa from 1983-2107. They are distinguishable from each other and from the subsequent modes according to the North et al. (1982) criteria, and were selected for further analysis. To investigate the robustness of the patterns, we regressed the precipitation anomalies on the normalized PCs and we tested ~~testing~~ for statistical significance using a two-tailed t–test. The test is based on adjusted number of degrees of freedom of the PCs and the grid-point precipitation after accounting for autocorrelation:

$$N^{*} = N\frac{(1-r_1 r_2)}{(1+r_1 r_2)} \quad (2)$$

where N^* is the adjusted number of degrees of freedom; N is the length of the time series (N=35); r_1 and r_2 are the first-order autocorrelation coefficients of the two time series pair under consideration, respectively.

Next, we decomposed each PC time series $\alpha(t)$ into its trend and interannual variability components, respectively:

$$\alpha(t) = \alpha_{\Delta}(t) + \alpha_{\sigma}(t).\alpha_{noise}(t) \quad (3)$$

where $\alpha_{\Delta}(t)$ denotes linear trend and $\alpha_{\sigma}(t)$ the interannual variability component. As stated above, we determine the linear trend component using a least-squares fit, so that the stochastic climate noise $\alpha_{noise}(t)$ now scales the interannual variability component. Here values of $\alpha_{\sigma}(t)$ larger than a unit standard deviation (±σ) are considered strong interannual variations which exceed the background noise, and are the basis for the determination of wet and dry years (Table 2).

The global SST and atmospheric circulation patterns associated with the first two extended-EOF modes were investigated using composite analysis. The composites are for the positive (+σ) and negative (-σ) cases of the first two PCs. For each PC, we consider two sets of composite differences. One set is based on the raw PCs (and includes both trends and variability), the other set is based on the PCs and other datasets after removing the least-squares linear trends (Table 2).

We calculated the composites as the differences between the mean anomalies for the wet years and dry years; t~~T~~hat is, years in which the relevant PC is greater than +1σ *minus* the years less than -1σ divided by 2. The composites were tested for statistical difference between the wet and dry years using a two-tailed *t*-test. The number of cases in each category is generally small (ranging from 2 to 7) which translates to small degrees of freedom. As a result, we marked the 90% confidence level for the

composites. Using thresholds of ±0.80σ or ±0.90σ slightly increases the statistical significance but does not change our conclusions.

3. The leading precipitation patterns

Here we discuss the first two extended-EOF modes of JAS precipitation over West Africa, which account for about 33% of the variance. We discuss their spatial patterns, time evolution, the impacts of linear trends and sensitivity to the choice of starting dates from the drier mid-1980s to the wetter mid-1990s.

3.1 The first two extended-EOF modes

Figure 4 shows the spatial pattern of JAS precipitation anomalies over West Africa, as represented by the first two extended-EOF modes. The extended-EOF1 accounts for 20.56%, and displays a homogeneous band of precipitation anomalies over the Sahel region often defined as the region north of 10°N (Fig. 4a-i). This pattern is quite coherent and statistically significant across the entire Sahel region in all datasets. To the south of the Sahel, there are opposite anomalies over the Guinea Coast. However, there are generally stronger anomalies across the entire Sahel when compared to the Guinea Coast. Thus, we refer to the extended-EOF1 as the Sahel mode hereafter. The extended-EOF2 which accounts for 12.75% of the variance shows robust precipitation anomalies that are generally confined to the Guinea Coast region (Fig. 1j-r). As a result, the extended-EOF2 is referred to as the Guinea Coast mode hereafter.

PC1 which represents the time evolution of the Sahel mode (that is, extended-EOF1), shows a strong upward inclination when considering both trend and variability (Fig. 5a). The values are generally above the zero line since the mid-2000s. In contrast, PC2 time series which corresponds to the Guinea Coast mode shows a discernible downward inclination.

The PC1 has a linear trend of 2.43 standard deviations per 35-year, and this is statistically significant at the 95% confidence level. This positive trend indicates a net monotonic increase in precipitation over the Sahel from 1983 to 2017 (Fig. 5c). The R^2 for the trend estimate (calculated from the regression of the PC1 on the time function) is 0.49, implying that 49% of the PC1 variance is explained by trend in our observational ensemble. PC2 has a negative trend of -1.25 standard deviations per 35-year, suggesting a decline in precipitation over the Guinea Coast from 1983 to 2017 (Fig. 5d). However, the PC2 explained variance of 13% is comparatively small (compared to that of PC1), and this trend is not statistically significant. After removing these linear trends from the raw PCs, the residual which represents the variability component is shown in Fig. 5e,f.

3.2 Relating the extended-EOF1 and linear trend

The foregoing analysis shows an ~~monotonic~~ increase in the JAS precipitation over the Sahel, but a decrease ~~occurred~~ over parts of the Guinea Coast from 1983-2017. To illustrate further the roles of monotonic trends for the region's precipitation, we also calculated the least-squares linear trend of the precipitation maps and compare it with the extended-EOF1 pattern. The trend map was estimated based on a normalized time function for a direct comparison with the extended-EOF1. We also accounted for autocorrelations in determining the number of degrees of freedom (see section 2.3).

Here we show both extended-EOF1 (Fig. 6a) and linear trend (Fig. 6b) maps using the multiple data ensemble-means. The two maps are remarkably similar with a pattern correlation of 0.93. Consistent with the extended-EOF1, the linear trend map displays a spatially coherent increases over the the Sahel. Indeed, the trend analysis displays a more robust decrease in precipitation over the Guinea Coast.

3.3 Sensitivity to the choice of starting dates

Linear trend estimates can be sensitive to the starting and ending dates used in analysis, given the broad range of periodicities observed in this region (Moron, 1997). Specifically, 1983 at the start of our analysis is considered to be very dry over West Africa, followed by wetter conditions in the mid-1990s (Fig. 5a,b; Fontaine et al., 2011;Lélé et al, 2015; Nicholson et al., 2018). We therefore investigate the sensitivity of this analysis to starting dates, between 1983 and 1995. We do this using three different statistics: pattern correlations between ensemble-means of the extended-EOF1 and trend maps, PC1 trends and PC1 variances explained by trends for chunks of the data (Fig. 7).

As shown in Fig. 7a, there is a close similarity in the time evolution of the pattern correlations, trends and explained variances. This implies that a large trend explains a large variance and the spatial patterns of the extended-EOF1 and trend maps closely matched. In addition to an overall downward inclination, the three statistics display decadal variations with maxima (minimum) from 1983-1985 (1988) and 1989-1990 (1994) to 2017. A comparison of these two epochs is based on the 95% confidence limit, estimated as 2σ (Fig. 7b-d).

The pattern correlation of 0.93 for 1983-2017 which forms the basis of our study falls with 2σ of the trends for all the chunks (0.89 ± 0.06). The same is true of the PC1 trend, which is statistically significant for all chunks, and PC1 variance explained by trends. The explained variance corresponds to $39\pm14\%$. Thus, 25-53% of the JAS precipitation over the Sahel from 1983-1995 to 2017 is attributable to linear trends. The spread of these quantities implies that the trend estimates are indeed influenced by interannual and decadal variability.

4. Related ocean-atmosphere teleconnections

In this section, we investigate the ocean-atmosphere teleconnections associated with the two leading modes of JAS precipitation over West Africa. We first consider the SST anomalies and then the

associated atmospheric circulation that can be directly linked to the precipitation anomalies. Composite analysis is used to distinguish between the patterns resulting purely from interannual variations (based on linearly detrended data) and those influenced by linear trends (see Table 2).

4.1 Related SST patterns

The Sahel mode is associated with anomalous warm SST anomalies over the North Atlantic (Fig. 8a). There is also strong warming in the Mediterranean Sea, consistent with previous studies (Gaetani et al., 2010; Park et al., 2016; Rowell, 2003), and western Indian Ocean, as well a cold blob in the subpolar gyre region of the North Atlantic which may represent the so-called warming hole (Caesar et al., 2018; Drijfhout et al., 2012; Rahmstorf et al., 2015). In the North Pacific, there is a robust SST pattern that is reminiscent of a negative phase of Pacific decadal variability (Liu and Di Lorenzo, 2018; Newman et al., 2016).

Generally speaking, the North Pacific, North Atlantic and Mediteranean SST anomalies associated with the Sahel pattern are qualitatively similar whether or not the linear trends are removed (Figs, 8a, c). The same is true of the warming hole in the North Atlantic. But consistent with precipitation over West Africa (Akinsanola et al., 2020; Diedhiou et al., 2018), the inclusion of trends appear to amplify the related SST anomalies (Fig. 8a,c).

For the Guinea Coast mode, there is a dipole structure with warm SST anomalies in the Atlantic Niño region and cold anomalies off Brazil-Uruguay-Argentina coast (Fig. 8b). This pattern corresponds to the positive phase of the South Atlantic Ocean dipole (SAOD) which is strongly correlated with Atlantic Niño, peaking during the northern hemisphere summer, and is also closely related to the winter pattern (Nnamchi el at., 2017; Morioka et al., 2011; Santis et al., 2020; Sun et al., 2017; Wainer et al., 2021; Venegas et al., 1996; 1997). In addition, the tropical Pacific is dominated by robust cold anomalies that are most pronounced in the central equatorial Pacific. These patterns are seen after

removing the linear trends, but the SST anomalies appears to be less robust (Fig. 8d). Previous studies discussed a two-way interaction between the equatorial Atlantic and Pacific (Cai et al., 2019; Jansen et al., 2009; Latif and Barnett, 1995), and this analysis suggests that such interactions are important for precipitation variability at the Guinea Coast.

Focusing on those regions with robust SST anomalies, we investigate the seasonal evolution of the SST indices associated with the Sahel and Guinea Coast modes, respectively (Figs. 8, 9, 10). The regions used to define the SST indices are indicated in Table 3. When considering both trends and variability, the North Atlantic, tropical southwest Indian Ocean, Mediterranean, and North Pacific SST indices increase progressively during the course of the year, with a peak in August (Fig. 9a) similar to the Sahel precipitation (Fig. 9c). Note that the NA-GTI (North Atlantic–global tropics SST index) discussed by Giannini et al. (2013) is strongly consistent with the North Atlantic index, implying that warm anomalies elsewhere in the tropics are overwhelmed by the equatorial Pacific cold anomalies. The cooling in the North Atlantic warming hole region also peaks in August. However, the curves show some slight variations with all indices exhibiting less robustness, after removing the linear trends (Fig. 9b,d).

The Atlantic Niño peaks in June (Fig. 10a,b), and leads the maximum precipitation anomalies at the Guinea Coast in August (Fig. 10c,d), which represents a two-month time lag. This connection is largely similar whether or not the linear trend is included in the analysis. The SAOD peaks in July but also displays a smaller peak in March. The peak in March may be related to variability of the St. Helena subtropical anticyclone which leads changes in the southeasterly trade winds and equatorial Atlantic SSTs (Lübbecke et al., 2010; Nnamchi et al., 2016), and is strongly influenced by linear trends. When considering both trends and variability, the Niño4 index shows a robust but generally flat curve (Fig. 10a). The Niño3 and Niño3.4 are strong only between April and June. This analysis suggests that the related robust cold anomalies emerge across the equatorial Pacific during the northern hemisphere

spring and early summer, and persist in the central part of the basin until late summer. However, the robustness of the equatorial Pacific anomalies generally decline after removing the linear trends (Fig. 10b).

The link between summer precipitation over West Africa and global SST anomalies undergoes decadal variations (Giannini et al., 2003; Rodríguez-Fonseca et al., 2015). For instance, our analysis of on the during the Sahel recovery period shows warm SST anomalies in the tropical southwest Indian Ocean. This implies a reversal of the cold anomalies in that region associated with Sahel drying trend during the 1930-2000 period (Giannini et al., 2003).

4.2 Related atmospheric circulation patterns

Precipitation over West Africa exhibits a strong annual cycle which is related to the north-south movements of the mean convection and precipitation belt associated with the monsoon system. We investigate the connection between convection and precipitation anomalies using OLR as a proxy for atmospheric convection (Stechmann and Ogrosky, 2014). Strong atmospheric convection is associated with elevated and cold cloud tops, and consequently reduced infrared radiation emission into space. Thus, negative (Positive) OLR anomalies denote enhanced (suppressed) convection and increased (decrease) cloud coverage. Indeed, EOF analysis of the OLR data yielded patterns reminiscent of the Sahel and Guinea Coast modes (not shown). Composite OLR anomalies are shown for the Sahel and Guinea Coast modes (Fig. 11) based on the years in Table 2.

The Sahel mode can be linked to intensified convection, represented by negative OLR anomalies, to the north of the mean ITCZ belt, indicated here by the maximum climatological-mean precipitation (Fig. 11a). A deep penetration of the convection belt over the Sahel is consistent with warm SST anomalies over North Atlantic (Fig. 8). The anomalous convection belt, which is seen across

the continent from Senegal to Ethiopia, is somewhat weakened when the linear trends are removed (Fig. 11c).

In contrast, the Guinea Coast summer precipitation anomalies can be associated with an unusually southerly location of the ITCZ (Fig. 11b,d), which is key to the growth of ocean-atmosphere anomalies over the equatorial Atlantic, and is consistent with the Atlantic Niño pattern (Fig. 8; Nnamchi et al., 2021; Richter et al., 2017). In this case, negative OLR anomalies are particularly strong close to the equator, south of the climatological maximum precipitation which denotes the mean ITCZ position. The negative OLR anomalies also occur over the northern parts of South America, consistent with the anomalous equatorial Atlantic warming (Fig. 8; Vallès-Casanova et al., 2020). The OLR anomalies associated with the Guinea Coast mode are quite robust whether or not the linear trends are included in the analysis.

Using the composites of the velocity potential and divergent/convergent winds in the lower (925 hPa) and upper troposphere (200 hPa), the OLR anomalies are linked to the large-scale convergence necessary for the precipitation anomalies (Fig. 12). Both the Sahel and Guinea Coast modes are associated with strong surface convergence compensated by divergence at the upper levels over West Africa. As expected, the maximum anomalous velocity potential and the convergence/divergence vectors occur at the coast for the Guinea Coast mode (Fig. 12b,d,f,h) but there is deeper penetration for the Sahel mode (Fig. 12a,c,e,g).

At both atmospheric levels, convergence (divergence) over the Sahel tends to be horizontally compensated by divergence (convergence) over South America (Fig. 12a,c,e,g). This implies a modification of the Walker Circulation, with a strengthening of the rising cell over Africa and a weakening of the rising cell over South America, associated with the Sahel mode. Note that the rising (sinking) cells of the mean Walker Circulation occur over the continents (oceans). The northward

penetration of the ITCZ which leads to increased precipitation over the Sahel, also causes dry conditions over South America, particularly the Northeast Brazil (Chang et al., 1997; Foltź et al., 2019; Servain, 1991). On the other hand, the southerly displacement of the ITCZ, convection, upper-level divergence and surface convergence associated with the Guinea Coast mode tend to extend across the equatorial Atlantic (Fig. 12b,d,f,h). This African-Atlantic pattern is horizontally compensated by strong surface divergence and upper-level convergence over the equatorial Pacific, implying a strengthening of the sinking Walker Cell in that region, and can be linked to the cold SST anomalies there (Fig. 8).

The foregoing clearly illustrates the importance of interactions between meridional (displacements of the ITCZ) and zonal (variations of the Walker Circulation) atmospheric circulations for both the Sahel and Guinea Coast modes.

5. Summary and conclusions

Based on an ensemble of nine precipitation datasets, derived from rain-gauge measurements or a combination of rain-gauge and satellite measurements, we show the leading patterns of the JAS precipitation over West Africa during the satellite-era 1983-2017. The extended-EOF1, representing the Sahel mode, displays a coherent increases in precipitation over much of West Africa and a decrease at the Guinea Coast. This Sahel pattern is closely reproduced using linear trend analysis. Linear trends explain 49% variance of the Sahel mode 1983-2017, with sensitivity of 25-53% to the choice of starting dates from the drier mid-1980s to the wetter mid-1990s. This sensitivity reflects the impacts of interannual and decadal variability on the trend estimates.

The extended-EOF2, the Guinea Coast mode, displays summer precipitation anomalies south of the Sahel. This mode is characterized by strong interannual variability, with statistically non-significant monotonic trends. Historical observations (Nicholson et al., 2018) and climate model simulation for the last millennium from 850 to 1850 CE (Zhang et al., 2021) show smaller trends for the Guinea Coast

compared to strong drying of the Sahel. Due to the strong interplay between trends and variability, it is necessary to better understand the future transition from the current wetting trend.

The leading precipitation patterns are linked to distinct SST and atmospheric anomalies. The Sahel mode is associated with warm anomalies in the North Atlantic, Mediterranean Sea and tropical southwest Indian Ocean as well as cold blob in the subpolar gyre region of North Atlantic. These patterns are amplified by linear trends, consistent with the hypothesis that the interactions of internal variability and external forcing were important for the Sahel precipitation recovery (Giannini and Kaplan, 2019). Furthermore, the Indian Ocean pattern denotes a reversal of cold anomalies in that region associated with a Sahel dry trend from 1930-2000, and underscores the possible roles of oceanic decadal variability (Giannini et al., 2003; Rodríguez-Fonseca et al., 2015).

The Guinea Coast mode is associated with Atlantic Niño SST anomalies at a time-lag of 2 months, and strong equatorial Pacific cooling. This time-lag is quite interesting, given that variability in precipitation leads that in the SST over the Atlantic Niño region (Nnamchi et al., 2021), and its source demands further investigation.

Our results highlight the importance of the interactions between meridional (north-south displacements of the ITCZ) and zonal (variations in the Walker Circulation) atmospheric circulation for the Sahel and Guinea Coast modes. In particular, the southerly displacement of the ITCZ, convection, upper-level divergence and surface convergence associated with the Guinea Coast mode are horizontally compensated by strong surface divergence and upper-level convergence over the equatorial Pacific where anomalous cooling prevails, implying a strong role for the Walker circulation. As seasonal prediction of the equatorial Atlantic climate remains a challenge (Counillon et al., 2021; Richter et al., 2018; 2020), the persistence of this ocean-atmosphere teleconnections from the equatorial Pacific may provide new insights.

Acknowledgments

H.C.N. was funded by the Deutsche Forschungs Gemeinschaft (DFG) project "NOVEL" through grant 456490637. V.N.D. was supported by the Chinese Academy of Sciences President's International Fellowship Initiative (CAS-PIFI). We thank anonymous reviewers for their thoughtful comments.

Author Contributions

H.C.N: Conceptualization, Methodology, Software, Formal Analysis, Visualization, Writing - Original Draft, Writing - Review & Editing.

V.N.D: Methodology, Software, Formal Analysis, Visualization, Writing - Review & Editing.

A.A.A: Methodology, Software, Formal Analysis, Visualization, Writing - Review & Editing.

U.K.O: Methodology, Writing - Review & Editing.

Data Availability

Datasets analyzed are referenced in Table 1 and can be found at the following publicly available sources:

ARC2:http://iridl.ldeo.columbia.edu/SOURCES/.NOAA/.NCEP/.CPC/.FEWS/.Africa/.DAILY/.ARC2/
CHIRPS: https://data.chc.ucsb.edu/products/CHIRPS-2.0/
CMAP:https://psl.noaa.gov/data/gridded/data.cmap.html
CPC: https://psl.noaa.gov/data/gridded/data.cpc.globalprecip.html
CRU:https://crudata.uea.ac.uk/cru/data/hrg/
GPCC: doi: 10.5676/DWD_GPCC/FD_M_V2018_025
GPCP: https://psl.noaa.gov/data/gridded/data.gpcp.html
PRECL: https://psl.noaa.gov/data/gridded/data.precl.html
UDEL: https://psl.noaa.gov/data/gridded/data.UDel_AirT_Precip.html

References

Adler, R.F., Huffman, G.J., Chang, A., Ferraro, R., Xie, P.-P., Janowiak, J., Rudolf, B., Schneider, U., Curtis, S., Bolvin, D., Gruber, A., Susskind, J., Arkin, P., Nelkin, E., 2003. The Version-2 Global Precipitation Climatology Project (GPCP) Monthly Precipitation Analysis (1979–Present). J. Hydrometeorol. 4, 1147–1167.

https://doi.org/10.1175/1525- 7541(2003)004<1147:TVGPCP>2.0.CO;2

Akinsanola, A.A., Ajayi, V.O., Adejare, A.T., Adeyeri, O.E., Gbode, I.E., Ogunjobi, K.O., Nikulin, G., Abolude, A.T., 2018. Evaluation of rainfall simulations over West Africa in dynamically

downscaled CMIP5 global circulation models. Theor. Appl. Climatol. 132, 437–450. https://doi.org/10.1007/s00704-017-2087-8

Akinsanola, A.A., Zhou, W. 2019. Dynamic and thermodynamic factors controlling increasing summer monsoon rainfall over the West African Sahel. *Clim Dyn* **52,** 4501–4514). https://doi.org/10.1007/s00382-018-4394-xAkinsanola, A.A., Ogunjobi, K.O., Ajayi, V.O., Adefisan, E.A., Omotosho, J.A., Sanogo, S., 2016. Comparison of five gridded precipitation products at climatological scales over West Africa. Meteorology and Atmospheric Physics 129(6), 669-689. https://doi.org/10.1007/s00703-016-0493-6.Atiah, W.A., Tsidu, G.M. and Amekudzi, L.K., 2020. Investigating the merits of gauge and satellite rainfall data at local scales in Ghana, West Africa. *Weather and Climate Extremes*, 30: 100292.

Bader, J., Latif, M., 2003. The impact of decadal-scale Indian Ocean sea surface temperature anomalies on Sahelian rainfall and the North Atlantic Oscillation. *Geophys. Res. Lett.* 30. https://doi.org/https://doi.org/10.1029/2003GL018426

Balas, N., Nicholson, S.E., Klotter, D., 2007. The relationship of rainfall variability in West Central Africa to sea-surface temperature fluctuations. *Int. J. Climatol.* https://doi.org/10.1002/joc.1456

Becker, A., Finger, P., Meyer-Christoffer, A., Rudolf, B., Schamm, K., Schneider, U., Ziese, M., 2013. A description of the global land-surface precipitation data products of the Global Precipitation Climatology Centre with sample applications including centennial (trend) analysis from 1901-present. Earth Syst. Sci. Data 5, 71–99. https://doi.org/10.5194/essd-5-71-2013

Bellomo, K., Murphy, L.N., Cane, M.A., Clement, A.C., Polvani, L.M., 2018. Historical forcings as main drivers of the Atlantic multidecadal variability in the CESM large ensemble. *Clim. Dyn.* 50, 3687–3698. https://doi.org/10.1007/s00382-017-3834-3

Biasutti, M., 2019. Rainfall trends in the African Sahel: Characteristics, processes, and causes. *WIREs Clim. Chang.* 10, e591. https://doi.org/https://doi.org/10.1002/wcc.591

Biasutti, M., Giannini, A., 2006. Robust Sahel drying in response to late 20th century forcings. Geophys. Res. Lett. 33. https://doi.org/https://doi.org/10.1029/2006GL026067

Bichet, A., Diedhiou, A., 2018. West African Sahel has become wetter during the last 30 years, but dry spells are shorter and more frequent. *Clim. Res.* 75, 155–162.

Booth, B.B.B., Dunstone, N.J., Halloran, P.R., Andrews, T., Bellouin, N., 2012. Aerosols implicated as a prime driver of twentieth-century North Atlantic climate variability. Nature. https://doi.org/10.1038/nature10946

Caesar, L., Rahmstorf, S., Robinson, A., Feulner, G., Saba, V., 2018. Observed fingerprint of a weakening Atlantic Ocean overturning circulation. Nature 556, 191.

Cai, W., Wu, L., Lengaigne, M., Li, T., McGregor, S., Kug, J.-S., Yu, J.-Y., Stuecker, M.F., Santoso, A., Li, X., Ham, Y.-G., Chikamoto, Y., Ng, B., McPhaden, M.J., Du, Y., Dommenget, D., Jia, F., Kajtar, J.B., Keenlyside, N., Lin, X., Luo, J.-J., Martín-Rey, M., Ruprich-Robert, Y., Wang, G., Xie, S.-P., Yang, Y., Kang, S.M., Choi, J.-Y., Gan, B., Kim, G.-I., Kim, C.-E., Kim, S., Kim, J.-H., Chang, P., 2019. Pantropical climate interactions. Science (80-.). 363, eaav4236. https://doi.org/10.1126/science.aav4236

Cavalcante, R.B.L., Ferreira, D.B. da S., Pontes, P.R.M., Tedeschi, R.G., da Costa, C.P.W., de Souza, E.B., 2020. Evaluation of extreme rainfall indices from CHIRPS precipitation estimates over the Brazilian Amazonia. *Atmos. Res.* 238, 104879. https://doi.org/https://doi.org/10.1016/j.atmosres.2020.104879

Chang, P., Ji, L., Li, H., 1997. A decadal climate variation in the tropical Atlantic Ocean from thermodynamic air-sea interactions. Nature 385, 516–518. https://doi.org/10.1038/385516a0

Chen, M., Xie, P., Janowiak, J.E., Arkin, P.A., 2002. Global Land Precipitation: A 50-yr Monthly Analysis Based on Gauge Observations. J. Hydrometeorol. 3, 249–266. https://doi.org/10.1175/1525-7541(2002)003<0249:GLPAYM>2.0.CO;2

Chen, M., Xie, P., Janowiak, J.E., Arkin, P.A., 2002. Global Land Precipitation: A 50-yr Monthly Analysis Based on Gauge Observations. J. Hydrometeorol. 3, 249–266. https://doi.org/10.1175/1525-7541(2002)003<0249:GLPAYM>2.0.CO;2

Counillon, F., Keenlyside, N., Toniazzo, T., Koseki, S., Demissie, T., Bethke, I., Wang, Y., 2021. Relating model bias and prediction skill in the equatorial Atlantic. Clim. Dyn. https://doi.org/10.1007/s00382-020-05605-8

Diatta S, Fink A.H. 2014. Statistical relationship between remote climate indices and West African monsoon variability. *Int. J. Climatol.* 34: 3348–3367.

Drijfhout, S., Oldenborgh, G.J. V, Cimatoribus, A., 2012. Is a decline of AMOC causing the warming hole above the North Atlantic in observed and modeled warming patterns? J. Clim. 25, 8373–8379.

Druyan, L.M., 2011. Studies of 21st-century precipitation trends over West Africa. *Int. J. Climatol.* https://doi.org/10.1002/joc.2180

Dunning, C.M., Black, E.C.L., Allan, R.P., 2016. The onset and cessation of seasonal rainfall over Africa. J. Geophys. Res. Atmos. 121, 11,405-411,424. https://doi.org/https://doi.org/10.1002/2016JD025428

Foltź, G.R., Brandt, P., Richter, I., Rodriguez-fonseca, B., Hernandez, F., Dengler, M., Rodrigues, R.R., Schmidt, J.O., Yu, L., Lefevre, N., Da Cunha, L.C., McPhaden, M.J., Araujo Filho, M.C.,

Karstensen, J., Hahn, J., Martín-Rey, M., Patricola, C.M., Poli, P., Zuidema, P., Hummels, R., Perez, R.C., Hatje, V., Luebbecke, J., Polo, I., Lumpkin, R., Bourlès, B., Asuquo, F.E., Lehodey, P., Conchon, A., Chang, P., Dandin, P., Schmid, C., Sutton, A.J., Giordani, H., Xue, Y., Illig, S., Losada, T., Grodsky, S., Gasparin, F., Lee, T., Mohino, E., Nobre, P., Wanninkhof, R., Keenlyside, N.S., Garcon, V., Sanchez-Gomez, E., Nnamchi, H.C., Drevillon, M., Storto, A., Remy, E., Lazar, A., Speich, S., Goes, M.P., Dorrington, T., Johns, W.E., Moum, J.N., Robinson, C., Perruche, C., Souza, R.B., Gaye, A., Lopez-Parages, J., Monerie, P.-A., Castellanos, P., Benson, N.U., Hounkonnou, M.N., Duha, J.T., 2019. The tropical atlantic observing system. Front. Mar. Sci. 6. https://doi.org/10.3389/fmars.2019.00206

Fontaine, B., Roucou, P., Gaetani, M., Marteau, R., 2011. Recent changes in precipitation, ITCZ convection and northern tropical circulation over North Africa (1979-2007). *Int. J. Climatol.* https://doi.org/10.1002/joc.2108

Froidurot, S., Diedhiou, A., 2017. Characteristics of wet and dry spells in the West African monsoon system. *Atmos. Sci. Lett.* 18(3), 125–131. https://doi.org/10.1002/asl.734.

Gaetani, M., Fontaine, B., Roucou, P., Baldi, M., 2010. Influence of the Mediterranean Sea on the West African monsoon: Intraseasonal variability in numerical simulations. J. Geophys. Res. Atmos. 115. https://doi.org/https://doi.org/10.1029/2010JD014436

Giannini, A., Kaplan, A., 2019. The role of aerosols and greenhouse gases in Sahel drought and recovery. *Clim. Change* 152, 449–466. https://doi.org/10.1007/s10584-018-2341-9

Giannini, A., Saravanan, R., Chang, P., 2003. Oceanic Forcing of Sahel Rainfall on Interannual to Interdecadal Time Scales. *Science* (80-.). https://doi.org/10.1126/science.1089357

Giannini, A., R. Saravanan, and P. Chang. 2005. Dynamics of the boreal summer African monsoon in the NSIPPI atmospheric model. *Clim Dyn* 25, 517-535.

Giannini, A., Salack, S., Lodoun, T., Ali, A., Gaye, A.T., Ndiaye, O., 2013. A unifying view of climate change in the Sahel linking intra-seasonal, interannual and longer time scales. Environ. Res. Lett. 8, 24010. https://doi.org/10.1088/1748-9326/8/2/024010

Harris, I., Osborn, T.J., Jones, P., Lister, D., 2020. Version 4 of the CRU TS monthly high-resolution gridded multivariate climate dataset. Sci. Data 7, 109. https://doi.org/10.1038/s41597-020-0453-3

Haustein, K., Otto, F.E.L., Venema, V., Jacobs, P., Cowtan, K., Hausfather, Z., Way, R.G., White, B., Subramanian, A., Schurer, A.P., 2019. A Limited Role for Unforced Internal Variability in Twentieth-Century Warming. *J. Clim.* 32, 4893–4917. https://doi.org/10.1175/JCLI-D-18-0555.1

Held, I.M., Delworth, T.L., Lu, J., Findell, K.L., Knutson, T.R., 2005. Simulation of Sahel drought in the 20th and 21st centuries. *Proc. Natl. Acad. Sci.* 102, 17891–17896. https://doi.org/10.1073/pnas.0509057102

Hersbach, H., Bell, B., Berrisford, P., Hirahara, S., Horányi, A., Muñoz-Sabater, J., Nicolas, J., Peubey, C., Radu, R., Schepers, D., Simmons, A., Soci, C., Abdalla, S., Abellan, X., Balsamo, G., Bechtold, P., Biavati, G., Bidlot, J., Bonavita, M., De Chiara, G., Dahlgren, P., Dee, D., Diamantakis, M., Dragani, R., Flemming, J., Forbes, R., Fuentes, M., Geer, A., Haimberger, L., Healy, S., Hogan, R.J., Hólm, E., Janisková, M., Keeley, S., Laloyaux, P., Lopez, P., Lupu, C., Radnoti, G., de Rosnay, P., Rozum, I., Vamborg, F., Villaume, S., Thépaut, J.-N., 2020. The ERA5 global reanalysis. Q. J. R. Meteorol. Soc. n/a. https://doi.org/10.1002/qj.3803

Hewitson, B.C., Daron, J., Crane, R.G., Zermoglio, M.F., Jack, C., 2014. Interrogating empirical-statistical downscaling. *Clim. Change* 122, 539–554. https://doi.org/10.1007/s10584-013-1021-z

Jansen, M.F., Dommenget, D., Keenlyside, N., 2009. Tropical Atmosphere–Ocean Interactions in a Conceptual Framework. J. Clim. 22, 550–567. https://doi.org/10.1175/2008JCLI2243.1

Kang, S.M., Held, I.M., Frierson, D.M.W., Zhao, M., 2008. The Response of the ITCZ to Extratropical Thermal Forcing: Idealized Slab-Ocean Experiments with a GCM. J. Clim. 21, 3521–3532. https://doi.org/10.1175/2007JCLI2146.1

Latif, M., Barnett, T.P., 1995. Interactions of the Tropical Oceans. J. Clim. 8, 952–964. https://doi.org/10.1175/1520-0442(1995)008<0952:IOTTO>2.0.CO;2

Le Barbé, L., Lebel, T., Tapsoba, D., 2002. Rainfall variability in West Africa during the years 1950-90. *J. Clim.* https://doi.org/10.1175/1520-0442(2002)015<0187:RVIWAD>2.0.CO;2

Lebel, T., Ali, A., 2009. Recent trends in the Central and Western Sahel rainfall regime (1990-2007). *J. Hydrol.* https://doi.org/10.1016/j.jhydrol.2008.11.030

Legates, D.R., Willmott, C.J., 1990. Mean seasonal and spatial variability in gauge-corrected, global precipitation. Int. J. Climatol. 10, 111–127. https://doi.org/10.1002/joc.3370100202

Lélé, M.I., Leslie, L.M., 2016. Intraseasonal variability of low-level moisture transport over West Africa. *Clim. Dyn.* 47, 3575–3591. https://doi.org/10.1007/s00382-016-3334-x

Lélé, M.I., Leslie, L.M., Lamb, P.J., 2015. Analysis of Low-Level Atmospheric Moisture Transport Associated with the West African Monsoon. *J. Clim.* 28, 4414–4430. https://doi.org/10.1175/JCLI-D-14-00746.1

Liebmann, B., Bladé, I., Kiladis, G.N., Carvalho, L.M. V, Senay, G.B., Allured, D., Leroux, S., Funk, C., 2012. Seasonality of African Precipitation from 1996 to 2009. J. Clim. 25, 4304–4322. https://doi.org/10.1175/JCLI-D-11-00157.1

Liebmann, B., Smith, C.A., 1996. Description of a Complete (Interpolated) Outgoing Longwave Radiation Dataset. *Bull. Am. Meteorol. Soc.* 77, 1275–1277.

Liu, W., Cook, K.H., Vizy, E.K., 2019. Role of the West African westerly jet in the seasonal and diurnal cycles of precipitation over West Africa. Climate Dynamics 54(1-2), 843-861. https://doi.org/10.1007/s00382-019-05035-1.

Liu, Z., Di Lorenzo, E., 2018. Mechanisms and Predictability of Pacific Decadal Variability. Curr. Clim. Chang. Reports 4, 128–144. https://doi.org/10.1007/s40641-018-0090-5

Losada, T., Rodríguez-Fonseca, B., Kucharski, F., 2012. Tropical influence on the summer Mediterranean climate. *Atmos. Sci. Lett.* https://doi.org/10.1002/asl.359

Lübbecke, J.F., Böning, C.W., Keenlyside, N.S., Xie, S.-P., 2010. On the connection between Benguela and equatorial Atlantic Niños and the role of the South Atlantic Anticyclone. J. Geophys. Res. Ocean. 115. https://doi.org/10.1029/2009JC005964

Maloney, E.D., Shaman, J., 2008. Intraseasonal variability of the West African monsoon and Atlantic ITCZ. *J. Clim.* https://doi.org/10.1175/2007JCLI1999.1

Mohino, E., Janicot, S., Bader, J., 2011. Sahel rainfall and decadal to multi-decadal sea surface temperature variability. *Clim. Dyn.* https://doi.org/10.1007/s00382-010-0867-2

Moron, V., 1997. Trend, decadal and interannual variability in annual rainfall of subequatorial and tropical North Africa (1900–1994). Int. J. Climatol. 17, 785–805. https://doi.org/https://doi.org/10.1002/(SICI)1097-0088(19970630)17:8<785::AID-JOC153>3.0.CO;2-I

Nash, D.J., De Cort, G., Chase, B.M., Verschuren, D., Nicholson, S.E., Shanahan, T.M., Asrat, A., Lézine, A.M., Grab, S.W., 2016. African hydroclimatic variability during the last 2000 years. *Quat. Sci. Rev.* https://doi.org/10.1016/j.quascirev.2016.10.012

Newman, M., Alexander, M.A., Ault, T.R., Cobb, K.M., Deser, C., Di Lorenzo, E., Mantua, N.J., Miller, A.J., Minobe, S., Nakamura, H., Schneider, N., Vimont, D.J., Phillips, A.S., Scott, J.D., Smith, C.A., 2016. The Pacific Decadal Oscillation, Revisited. J. Clim. 29, 4399–4427. https://doi.org/10.1175/JCLI-D-15-0508.1

Nkrumah, F., Vischel, T., Panthou, G., Klutse, N.A.B., Adukpo, D.C., Diedhiou, A., 2019. Recent Trends in the Daily Rainfall Regime in Southern West Africa. *Atmosphere (Basel).* 10. https://doi.org/10.3390/atmos10120741

Nguyen, H., Thorncroft, C.D., Zhang, C., 2011. Guinean coastal rainfall of the West African Monsoon. Q. J. R. Meteorol. Soc. 137, 1828–1840. https://doi.org/10.1002/qj.867

Nicholson, S.E., 2008. The intensity, location and structure of the tropical rainbelt over west Africa as factors in interannual variability. *Int. J. Climatol*. https://doi.org/10.1002/joc.1507

Nicholson, S. E., and J. P. Grist, 2001. A conceptual model for understanding rainfall variability in the West Africa Sahel on interannual and interdecadal timescales. *Int. J. Climatol.*, 21, 1733-1757.

Nicholson, S.E., Webster, P.J., 2007. A physical basis for the interannual variability of rainfall in the Sahel. Q. J. R. Meteorol. Soc. https://doi.org/10.1002/qj.104

Nicholson, S.E., Funk, C., Fink, A.H., 2018. Rainfall over the African continent from the 19th through the 21st century. *Glob. Planet. Change* 165, 114–127. https://doi.org/10.1016/j.gloplacha.2017.12.014

Nnamchi, H.C., Li, J., 2016. Floods and droughts along the Guinea Coast in connection with the South Atlantic Dipole, in: Li, J., Swinbank, R., Grotjahn, R., Volkert, H. (Eds.), Dynamics and Predictability of Large-Scale, High-Impact Weather and Climate Events, Special Publications of the International Union of Geodesy and Geophysics. Cambridge University Press, pp. 271–279. https://doi.org/10.1017/CBO9781107775541.023

Nnamchi, H.C., Li, J., 2011. Influence of the South Atlantic Ocean dipole on West African summer precipitation. *J. Clim.* 24. https://doi.org/10.1175/2010JCLI3668.1

Nnamchi, H.C., Li, J., Kang, I.-S., Kucharski, F., 2013. Simulated impacts of the South Atlantic Ocean Dipole on summer precipitation at the Guinea Coast. *Clim. Dyn.* 41. https://doi.org/10.1007/s00382-012-1629-0

Nnamchi, Hyacinth C, Li, J., Kucharski, F., Kang, I.-S., Keenlyside, N.S., Chang, P., Farneti, R., 2016. An Equatorial–Extratropical Dipole Structure of the Atlantic Niño. J. Clim. 29, 7295–7311. https://doi.org/10.1175/JCLI-D-15-0894.1

Nnamchi, H.C., Latif, M., Keenlyside, N.S., Kjellsson, J., Richter, I., 2021. Diabatic heating governs the seasonality of the Atlantic Niño. *Nat. Commun.* 12, 376. https://doi.org/10.1038/s41467-020-20452-1

Novella, N.S., Thiaw, W.M., 2012. African Rainfall Climatology Version 2 for Famine Early Warning Systems. J. Appl. Meteorol. Climatol. 52, 588–606. https://doi.org/10.1175/JAMC-D-11-0238.1

North, G.R., Bell, T.L., Cahalan, R.F., Moeng, F.J., 1982. Sampling Errors in the Estimation of Empirical Orthogonal Functions. Mon. Weather Rev. 110, 699–706. https://doi.org/10.1175/1520-0493(1982)110<0699:SEITEO>2.0.CO;2

Okoro, U.K., Chen, W., Nath, D., Nnamchi, H.C., 2020. Variability and trends of atmospheric moisture in recent West African monsoon season and the Coordinated Regional Downscaling Experiment-Africa projected 21st century scenarios. *Int. J. Climatol.* 40(2), 1149-1163. https://doi.org/10.1002/joc.6261.

Pomposi, C., Kushnir, Y., Giannini, A., Biasutti, M., 2020. Toward Understanding the Occurrence of Both Wet and Dry Sahel Seasons during El Niño: The Modulating Role of the Global Ocean. J. Clim. 33, 1193–1207. https://doi.org/10.1175/JCLI-D-19-0219.1

Paeth H, Fink A. H.,Pohle S, Keis F, H. Machel and C. Samimi. 2011. Meteorological characteristics and potential causes of the 2007 flood in sub-Saharan Africa. *Int. J. Climatol.* 31: 1908–1926.

Park, J.Y., Bader, J., Matei, D., 2016. Anthropogenic Mediterranean warming essential driver for present and future Sahel rainfall. *Nat. Clim. Chang.* https://doi.org/10.1038/nclimate3065

Polo, I., B. Rodriguez-Fonseca, T. Losada, and J. Garcia-Serrano. 2008. Tropical Atlantic variability modes (1979–2002). Part I: Time-evolving SST modes related to West African rainfall. *J. Climate*, 21, 6457–6475

Rahmstorf, S., Box, J.E., Feulner, G., Mann, M.E., Robinson, A., Rutherford, S., Schaffernicht, E.J., 2015. Exceptional twentieth-century slowdown in Atlantic Ocean overturning circulation. Nat. Clim. Chang. https://doi.org/10.1038/nclimate2554

Reynolds, R.W., Rayner, N.A., Smith, T.M., Stokes, D.C., Wang, W., 2002. An Improved In Situ and Satellite SST Analysis for Climate. J. Clim. 15, 1609–1625. https://doi.org/10.1175/1520-0442(2002)015<1609:AIISAS>2.0.CO;2

Richter, I., Chang, P., Liu, X., 2020. Impact of Systematic GCM Errors on Prediction Skill as Estimated by Linear Inverse Modeling. J. Clim. 33, 10073–10095. https://doi.org/10.1175/JCLI-D-20-0209.1

Richter, I., Doi, T., Behera, S.K., Keenlyside, N., 2018. On the link between mean state biases and prediction skill in the tropics: an atmospheric perspective. Clim. Dyn. 50, 3355–3374. https://doi.org/10.1007/s00382-017-3809-4

Richter, I., Xie, S.-P., Morioka, Y., Doi, T., Taguchi, B., Behera, S., 2017. Phase locking of equatorial Atlantic variability through the seasonal migration of the ITCZ. *Clim. Dyn.* 48, 3615–3629. https://doi.org/10.1007/s00382-016-3289-y

Rodríguez-Fonseca, B., Mohino, E., Mechoso, C.R., Caminade, C., Biasutti, M., Gaetani, M., Garcia-Serrano, J., Vizy, E.K., Cook, K., Xue, Y., Polo, I., Losada, T., Druyan, L., Fontaine, B., Bader, J., Doblas-Reyes, F.J., Goddard, L., Janicot, S., Arribas, A., Lau, W., Colman, A., Vellinga, M., Rowell, D.P., Kucharski, F., Voldoire, A., 2015. Variability and Predictability of West African Droughts: A Review on the Role of Sea Surface Temperature Anomalies. *J. Clim.* 28, 4034–4060. https://doi.org/10.1175/JCLI-D-14-00130.1

Rotstayn, L.D., Lohmann, U., 2002. Tropical Rainfall Trends and the Indirect Aerosol Effect. J. Clim. 15, 2103–2116. https://doi.org/10.1175/1520-0442(2002)015<2103:TRTATI>2.0.CO;2

Rowell, D.P., 2003. The Impact of Mediterranean SSTs on the Sahelian Rainfall Season. J. Clim. 16, 849–862. https://doi.org/10.1175/1520-0442(2003)016<0849:TIOMSO>2.0.CO;2

Sanogo, S., Fink, A.H., Omotosho, J.A., Ba, A., Redl, R., Ermert, V., 2015. Spatio-temporal characteristics of the recent rainfall recovery in West Africa. *Int. J. Climatol.* 35, 4589–4605. https://doi.org/10.1002/joc.4309

Santis, W., Castellanos, P., Campos, E., 2020. Memory Effect of the Southern Atlantic Subtropical Dipole. J. Clim. 33, 7679–7696. https://doi.org/10.1175/JCLI-D-19-0745.1

Satge, F., Defrance, D., Sultan, B., Bonnet, M.P., Seyler, F., Rouche, N., Pierron, F., Paturel, J.E., 2020. Evaluation of 23 gridded precipitation datasets across West Africa. Journal of Hydrology 581, 124412. https://doi.org/10.1016/j.jhydrol.2019.124412.

Schneider, U., Becker, A., Finger, P., Meyer-Christoffer, A., Ziese, M., 2020. GPCC Full Data Monthly Product Version 2020 at 0.25°: Monthly Land-Surface Precipitation from Rain-Gauges built on GTS-based and Historical Data [WWW Document]. Glob. Precip. Climatol. Cent. https://doi.org/10.5676/DWD_GPCC/FD_M_V2020_025

Schneider, U., Finger, P., Meyer-Christoffer, A., Rustemeier, E., Ziese, M., Becker, A., 2017. Evaluating the hydrological cycle over land using the newly-corrected precipitation climatology from the Global Precipitation Climatology Centre (GPCC). Atmosphere (Basel). 8. https://doi.org/10.3390/atmos8030052

Servain, J., 1991. Simple climatic indices for the tropical Atlantic Ocean and some applications. J. Geophys. Res. https://doi.org/10.1029/91jc01046

Sobral, B.S., de Oliveira-Júnior, J.F., Alecrim, F., Gois, G., Muniz-Júnior, J.G., de Bodas Terassi, P.M., Pereira-Júnior, E.R., Lyra, G.B., Zeri, M., 2020. PERSIANN-CDR based characterization and trend analysis of annual rainfall in Rio De Janeiro State, Brazil. *Atmos. Res.* 238, 104873. https://doi.org/10.1016/J.ATMOSRES.2020.104873

Stechmann, S.N., Ogrosky, H.R., 2014. The Walker circulation, diabatic heating, and outgoing longwave radiation. *Geophys. Res. Lett.* 41, 9097–9105. https://doi.org/10.1002/2014GL062257

Steinig, S., Harlaß, J., Park, W., Latif, M., 2018. Sahel rainfall strength and onset improvements due to more realistic Atlantic cold tongue development in a climate model. *Sci. Rep*. 8, 2569. https://doi.org/10.1038/s41598-018-20904-1

Suliman, A.H.A., Awchi, T.A., Al-Mola, M., Shahid, S., 2020. Evaluation of remotely sensed precipitation sources for drought assessment in Semi-Arid Iraq. *Atmos. Res.* 242, 105007. https://doi.org/https://doi.org/10.1016/j.atmosres.2020.105007

Sultan, B., Baron, C., Dingkuhn, M., Sarr, B., Janicot, S., 2005. Agricultural impacts of large-scale variability of the West African monsoon. *Agric. For. Meteorol.* https://doi.org/10.1016/j.agrformet.2004.08.005

Sultan, B., Janicot, S., Diedhiou, A., 2003. The West African monsoon dynamics. Part I: Documentation of intraseasonal variability. *J. Clim.* https://doi.org/10.1175/1520-0442(2003)016<3389:TWAMDP>2.0.CO;2

Sultan, B., Janicot, S., 2003. The West African Monsoon Dynamics. Part II: The “Preonset” and “Onset” of the Summer Monsoon. J. Clim. 16, 3407–3427. https://doi.org/10.1175/1520-0442(2003)016<3407:TWAMDP>2.0.CO;2

Sun, X., Cook, K.H., Vizy, E.K., 2017. The South Atlantic Subtropical High: Climatology and Interannual Variability. J. Clim. 30, 3279–3296. https://doi.org/10.1175/JCLI-D-16-0705.1

Sylla, M.B., Dell'Aquila, A., Ruti, P.M., Giorgi, F., 2010. Simulation of the intraseasonal and the interannual variability of rainfall over West Africa with RegCM3 during the monsoon period. *Int. J. Climatol*. https://doi.org/10.1002/joc.2029

Sylla, M.B., Giorgi, F., Coppola, E. and Mariotti, L., 2013. Uncertainties in daily rainfall over Africa: assessment of gridded observation products and evaluation of a regional climate model simulation. International Journal of Climatology, 33(7): 1805-1817.

Sylla, M.B., Nikiema, P.M., Gibba, P., Kebe, I., Klutse, N.A.B., 2016. Climate change over West Africa: Recent trends and future projections, in: Adaptation to Climate Change and Variability in Rural West Africa. https://doi.org/10.1007/978-3-319-31499-0_3

Tokinaga, H., Xie, S.-P., 2011. Weakening of the equatorial Atlantic cold tongue over the past six decades. *Nat. Geosci.* 4, 222–226. https://doi.org/10.1038/ngeo1078

Vallès-Casanova, I., Lee, S.-K., Foltz, G.R., Pelegrí, J.L., 2020. On the Spatiotemporal Diversity of Atlantic Niño and Associated Rainfall Variability Over West Africa and South America. *Geophys. Res. Lett*. 47, e2020GL087108. https://doi.org/10.1029/2020GL087108

Wagner, R.G., Silva, A.M. Da, 1994. Surface conditions associated with anomalous rainfall in the Guinea coastal region. *Int. J. Climatol.*, 14: 179-199. https://doi.org/10.1002/joc.3370140205

Wainer, I., Prado, L.F., Khodri, M., Otto-Bliesner, B., 2021. The South Atlantic sub-tropical dipole mode since the last deglaciation and changes in rainfall. Clim. Dyn. 56, 109–122. https://doi.org/10.1007/s00382-020-05468-z

Washington, R., Harrison, M., Conway, D., Black, E., Challinor, A., Grimes, D., Jones, R., Morse, A., Kay, G., Todd, M., 2006. African climate change: Taking the shorter route. *Bull. Am. Meteorol. Soc.* https://doi.org/10.1175/BAMS-87-10-1355

Worou, K., Goose, H., Fichefet, T., Guichard, F., Diakhate, 2020. Interannual variability of rainfall in the Guinean Coast region and its links with sea surface temperature changes over the twentieth century for the different seasons. *Clim. Dyn.* https://doi.org/10.1007/s00382-020-05276-5.

Xie, P., Arkin, P.A., 1997. Global Precipitation : A 17-Year Monthly Analysis Based on Gauge Observations , Satellite Estimates , and Numerical Model Outputs. Bull. Amer. Meteor. Soc 2539–2558.

Yu, J., Li, X.-F., Lewis, E., Blenkinsop, S., Fowler, H.J., 2020. UKGrsHP: a UK high-resolution gauge–radar–satellite merged hourly precipitation analysis dataset. *Clim. Dyn.* 54, 2919–2940. https://doi.org/10.1007/s00382-020-05144-2

Zhang, Q., Berntell, E., Li, Q., Ljungqvist, F.C., 2021. Understanding the variability of the rainfall dipole in West Africa using the EC-Earth last millennium simulation. Clim. Dyn. https://doi.org/10.1007/s00382-021-05696-x

Zhao-Hui, L., Dike, V. N., 2018. Impact of Trans-Atlantic-Pacific Ocean Dipole–like pattern on summer precipitation variability over West Africa. *Atmos. Ocean. Sci. Lett.* 11, 509–517. https://doi.org/10.1080/16742834.2018.1529533

Table 1: The analyzed precipitation datasets

	Dataset	**Description**	**Resolution (Lat×Lon)**	**Reference**	**Estimate**
1.	ARC2	Africa Rainfall Climatology (ARC) precipitation estimates for Africa from the Famine Early Warning System	0.1° × 0.1°	Novella & Thiaw, 2012	Rain-gauge/Satellite
2.	CHIRPS	Climate Hazards Group InfraRed Precipitation with Station data (CHIRPS) precipitation	0.05°×0.05°	Funk et al., 2015	Rain-gauge/Satellite
3.	CMAP	CPC Merged Analysis of Precipitation	2.5°×2.5°	Xie & Arkin, 1997	Rain-gauge/Satellite
4.	CPC	CPC Global Precipitation	0.5°×0.5°	Chen et al., 2008	Rain-gauge/Satellite
5.	CRU	CRU TS4.03 Precipitation	0.5°×0.5°	Harris et al.,2020	Rain-gauge
6.	GPCC	GPCC full data monthly product version 2020	0.25°×0.25°	Schneider et al., 2018	Rain-gauge
7.	GPCP	GPCP Version 2.3 Combined Precipitation Dataset	2.5°×2.5°	Adler et al., 2003	Rain-gauge/Satellite
8.	PRECL	Precipitation Reconstruction over Land (PREC/L)	1.0°×1.0°	Chen et al., 2002	Rain-gauge
9.	UDEL	Univ. of Delaware Precipitation and Air Temp v5.01	1.0°×1.0°	Legates & Willmott, 1990	Rain-gauge

Table 2: The years selected for composite analysis, those selected with and without trends are in bold

	PC1	PC2
Trend + variability	[1994, **1999**, 2010, **2012,** 2015, 2016] *minus* [1983, **1984**, 1987, 1990, 1997, **2002**]	[**1985, 1987,**1988, **1989,** 1995, **1999, 2008**] *minus* [**1983, 1997, 2001, 2005,** 2013, 2015]
No trends	[1988, 1994, **1999**, **2012**] *minus* [**1984, 2002**]	[**1985, 1987, 1989, 1999, 2008,** 2016] *minus* [**1983, 1997, 2001, 2005]**

Table 3: Regions for calculation of the SST indices analyzed.

SST Index	**Region**
NA-GTI (North Atlantic *minus* global tropics index)	10-40°N, 15-75°W *minus* 20°S-20°N,180°W-180°E
Tropical southwest Indian Ocean	15°S-5°N,55°W-80°E
North Atlantic	5-40°N, 10-75°W
Mediterranean Sea	30-42°N, 5°W-25°E
North Atlantic warming hole	45-50°N, 15-35°W
North Pacific	35-45°N, 140°E-140°W
Atlantic Niño (Atl3)	3°S-3°N, 0-20°W
Niño3	5°S-5°N, 90-150°W
Niño3.4	5S-5°N, 120-170°W
Niño4	5S-5°N, 160°E-150°W

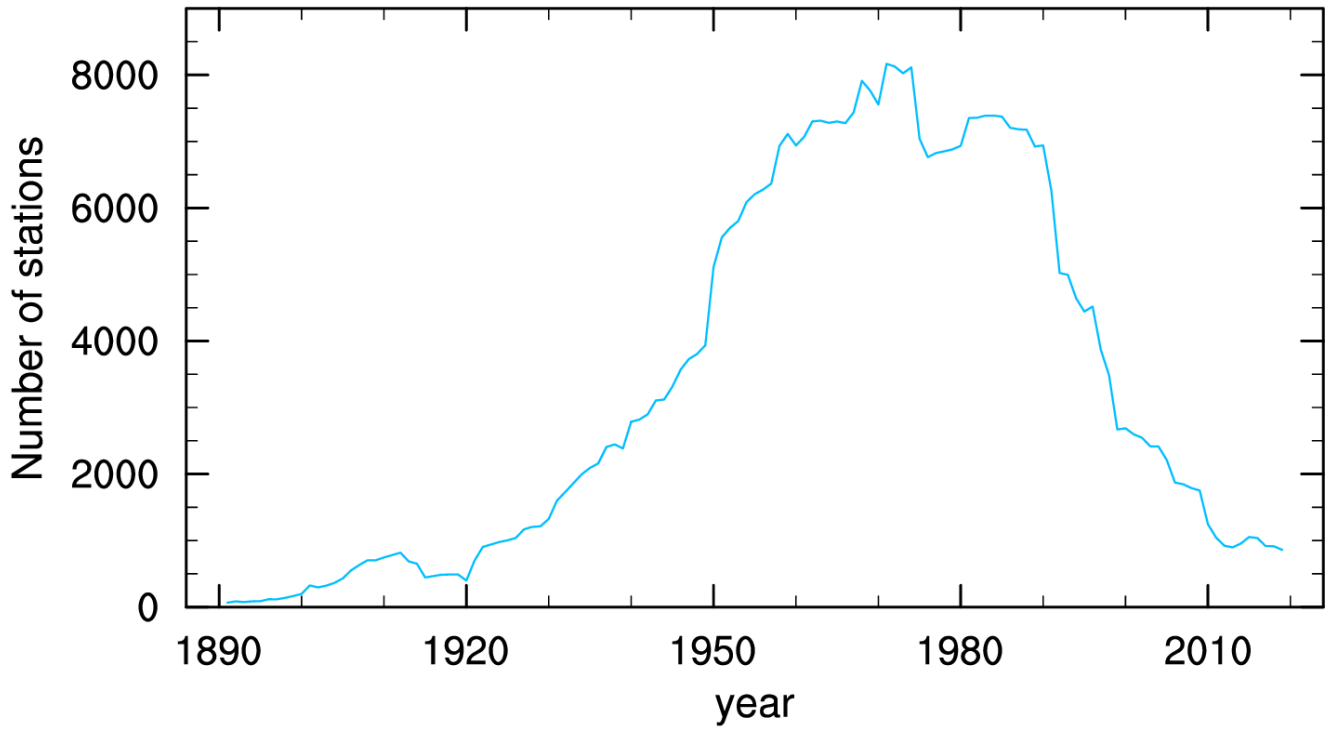

Fig. 1. Number of rain gauge stations over West Africa (0-20°N, 20°W-20°E) included in GPCC dataset (Schneider et al., 2020) from 1891 to 2019.

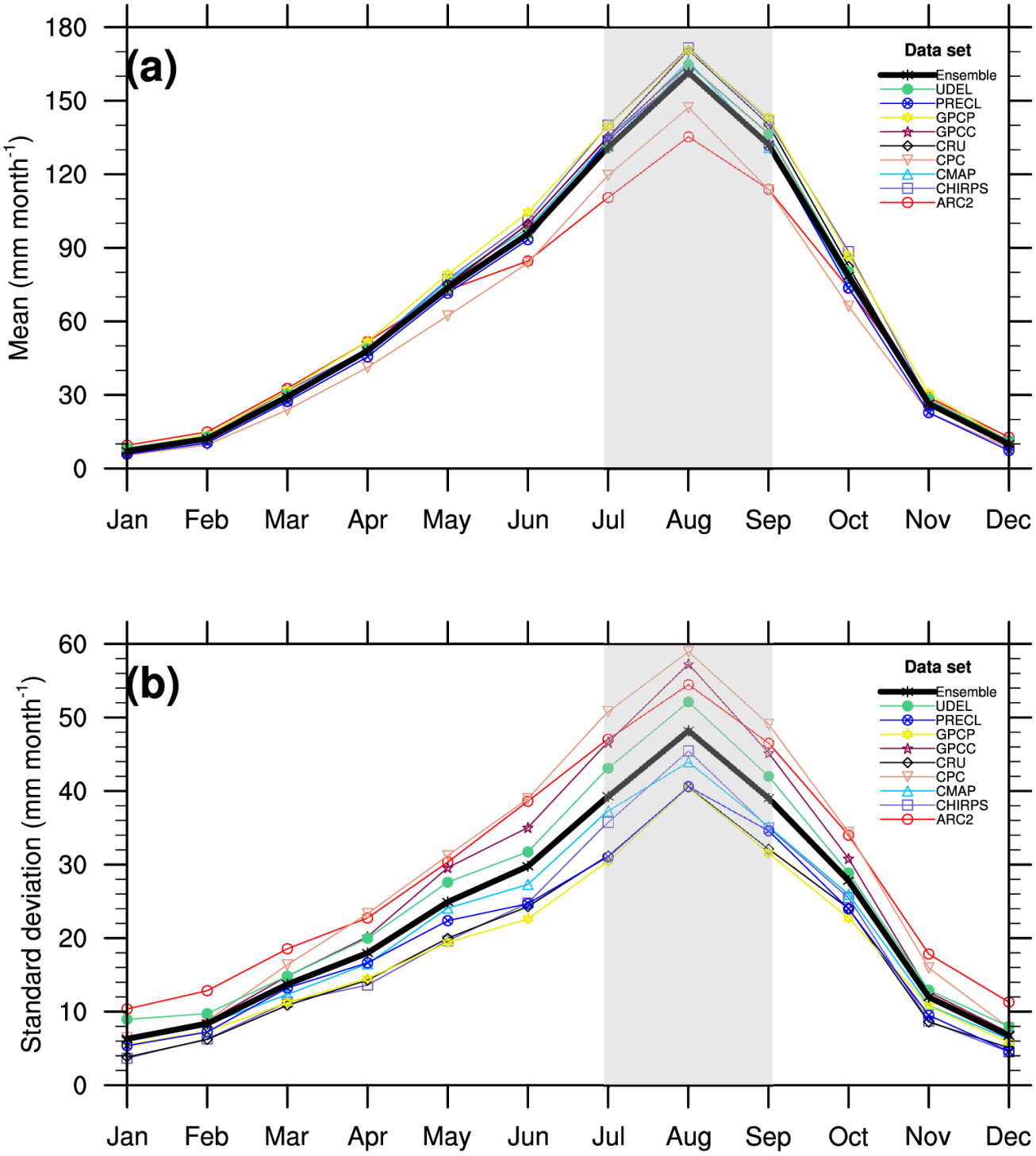

Fig. 2. Annual cycle of the (a) mean and (b) standard deviation of precipitation over averaged West Africa (0-20°N, 20°W-20°E) in the different data sets. In each panel, the vertical grey bar shows the July-August-September (JAS) that is further analyzed in this study.

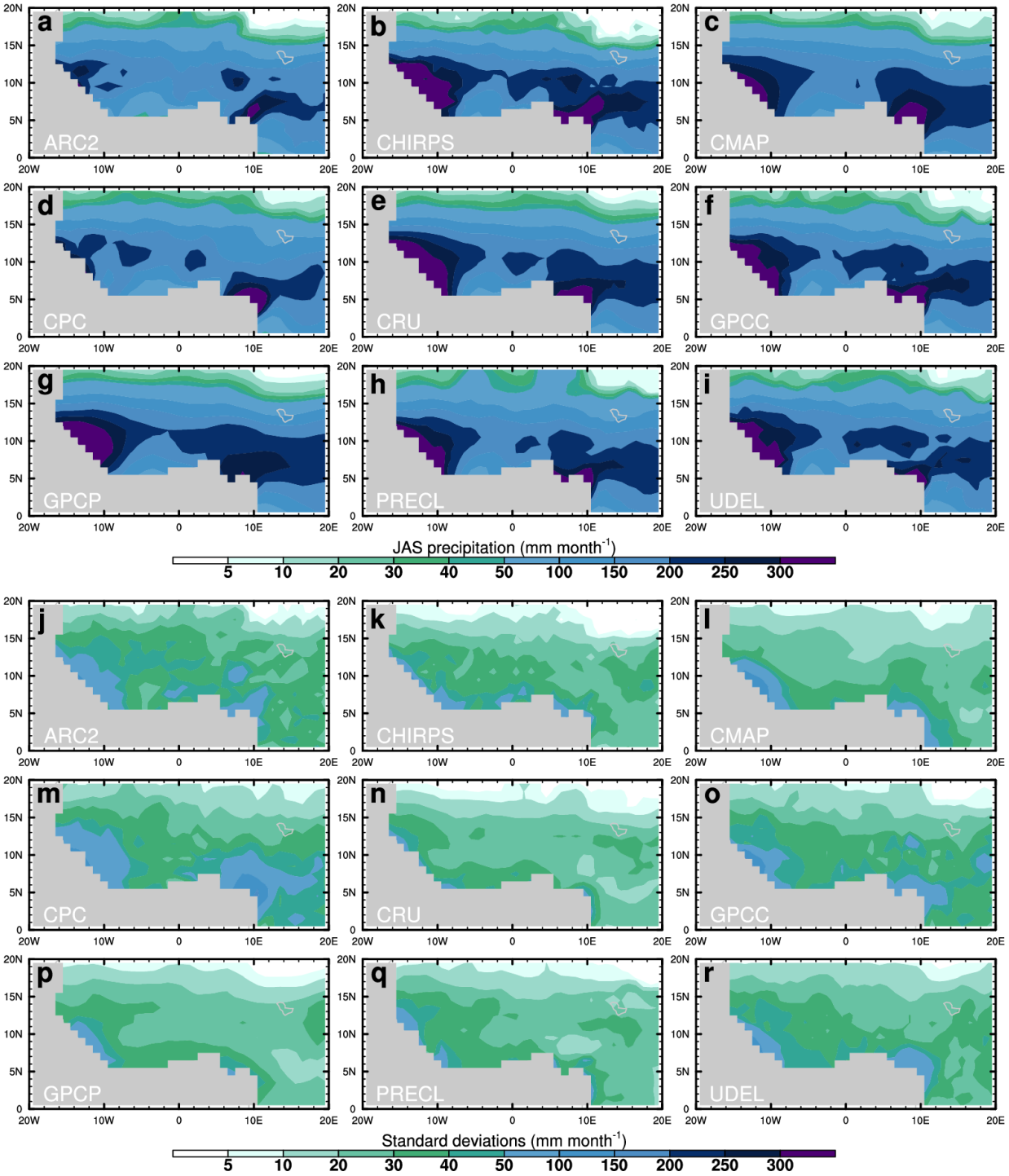
a
ARC2
b
CHIRPS
c
CMAP
d
CPC
e
CRU
f
GPCC
g
GPCP
h
PRECL
i
UDEL
JAS precipitation (mm month-1)
5 10 20 30 40 50 100 150 200 250 300
j
ARC2
k
CHIRPS
l
CMAP
m
CPC
n
CRU
o
GPCC
p
GPCP
q
PRECL
r
UDEL
Standard deviations (mm month-1)
5 10 20 30 40 50 100 150 200 250 300

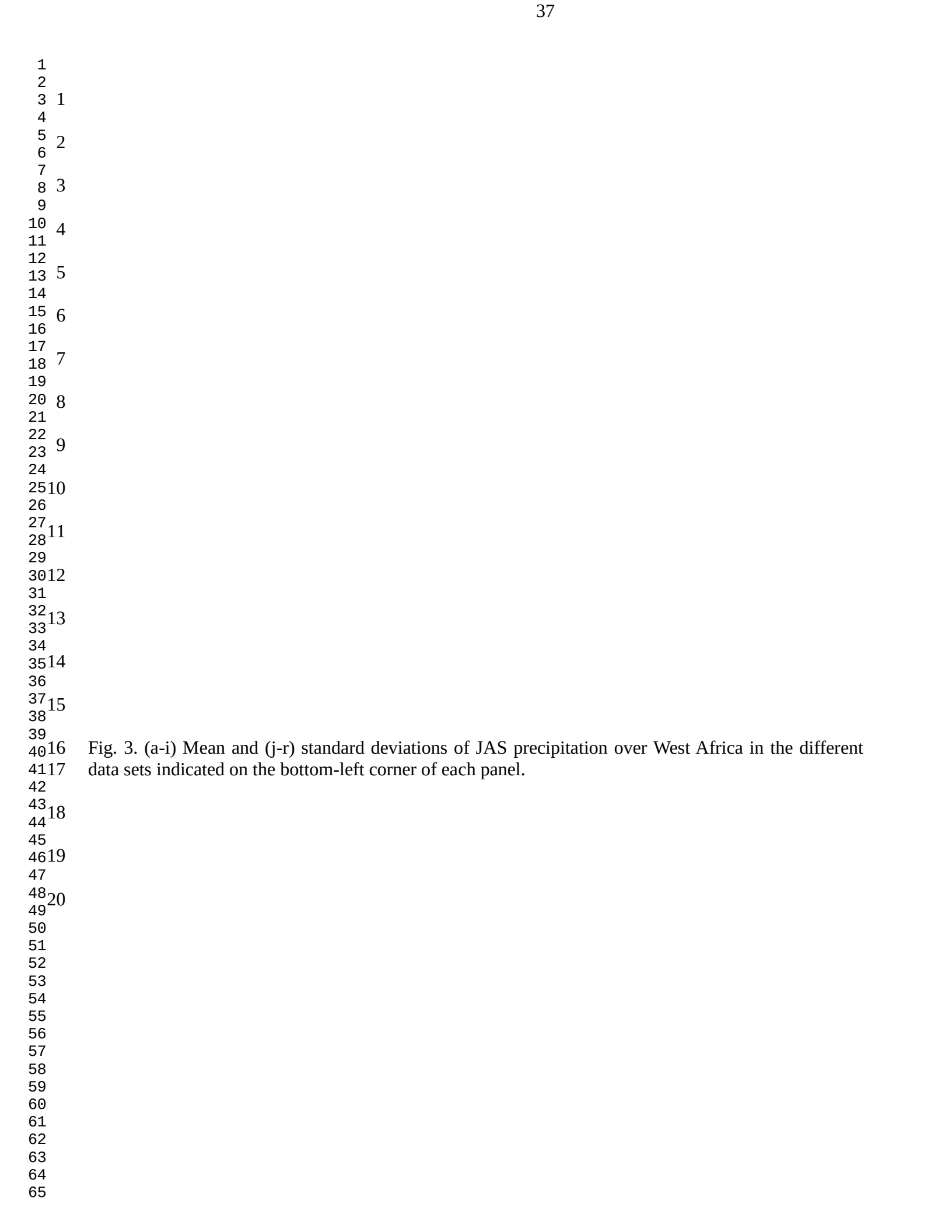

Fig. 3. (a-i) Mean and (j-r) standard deviations of JAS precipitation over West Africa in the different data sets indicated on the bottom-left corner of each panel.

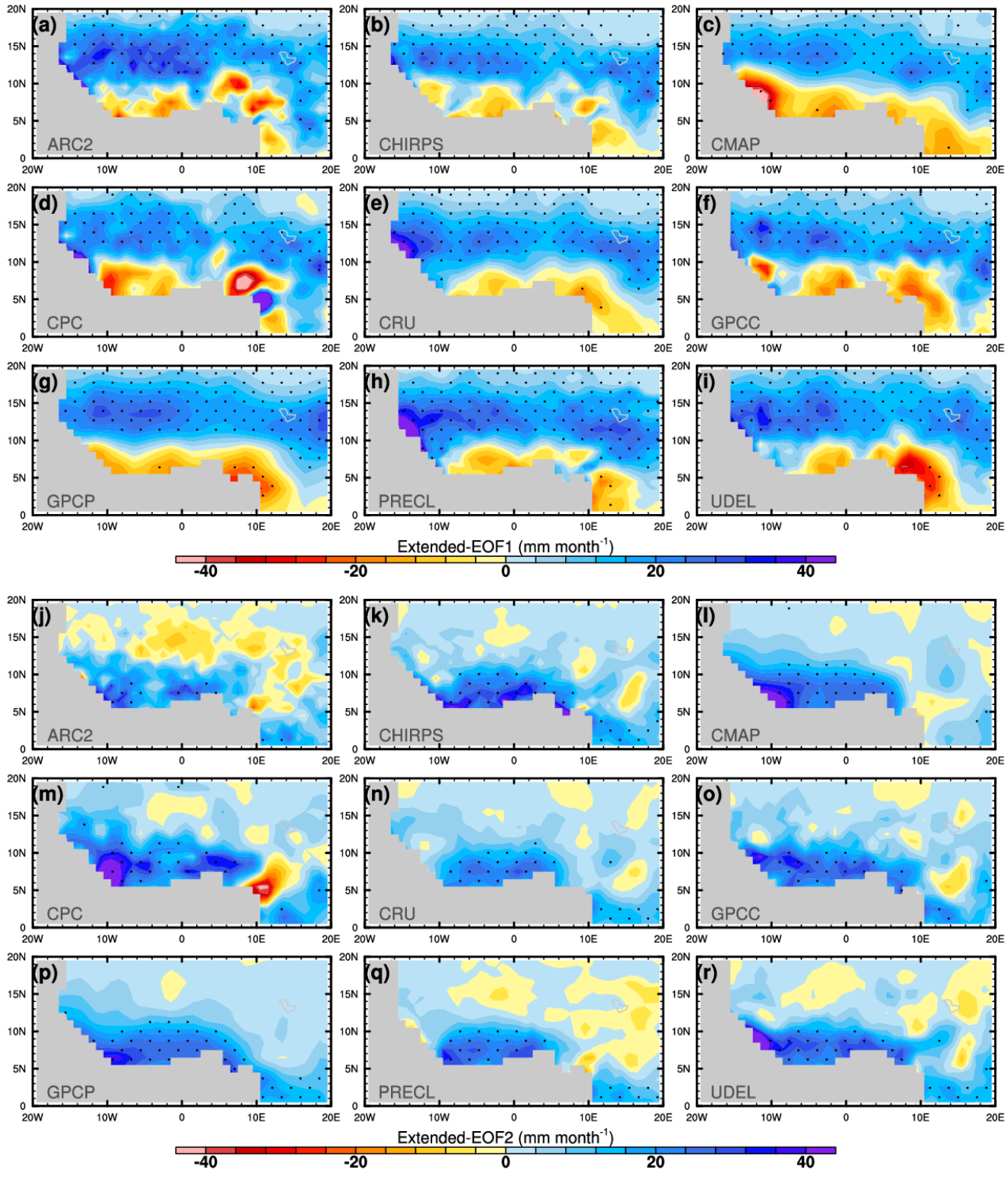

Fig. 4. Spatial patterns of the (a-i) ensemble-EOF1 and (j-r) ensemble-EOF2 of JAS precipitation over West Africa, obtained by regressing the JAS precipitation on the PC1 and PC2, respectively. The stipples denote statistical significance at the 95% confidence level.

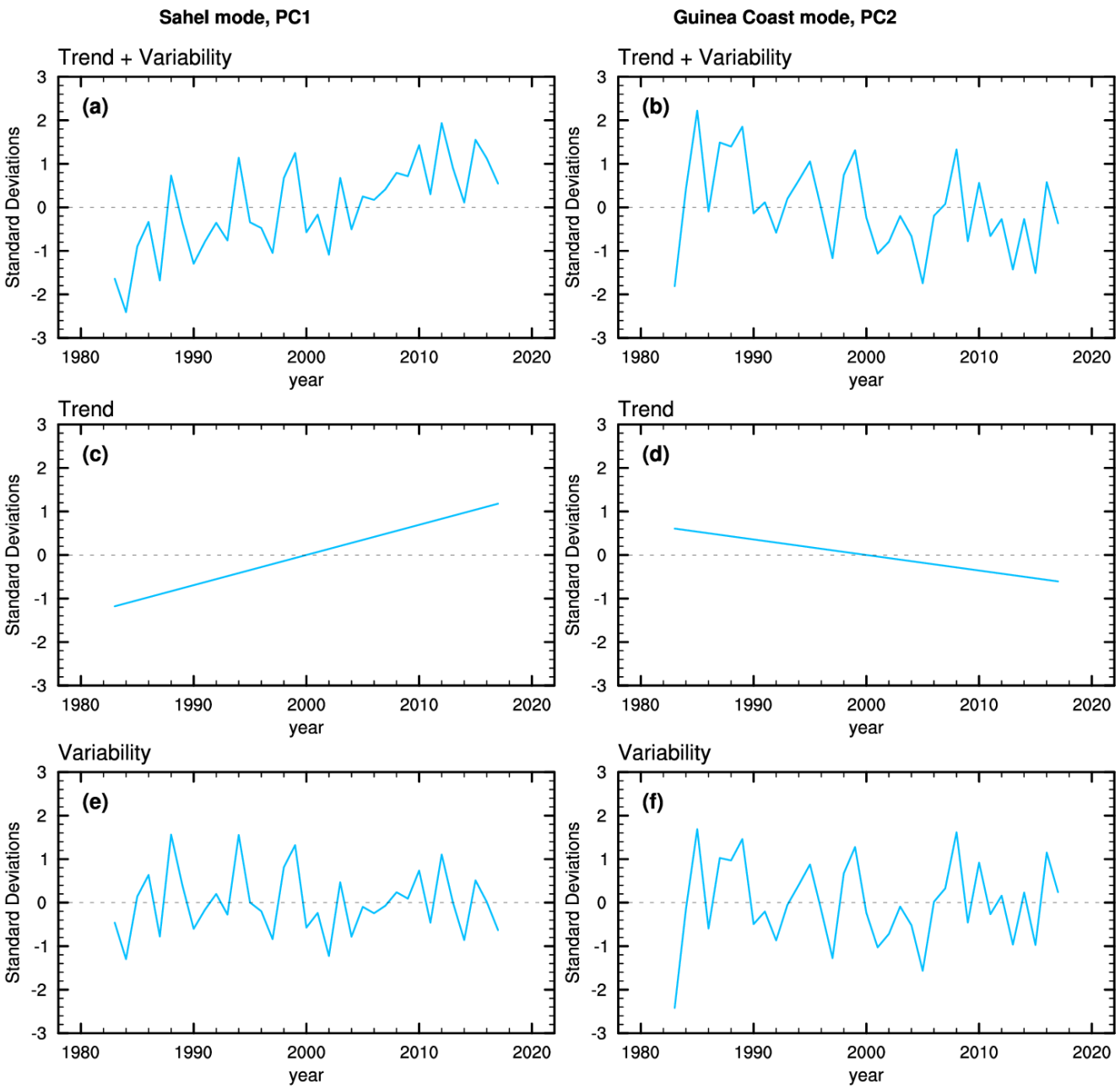

Fig. 5. (a) PC1 and (b) PC2 of the JAS precipitation over West Africa and their decompositions into the (c,d) linear trend and (e,f) interannual variability components.

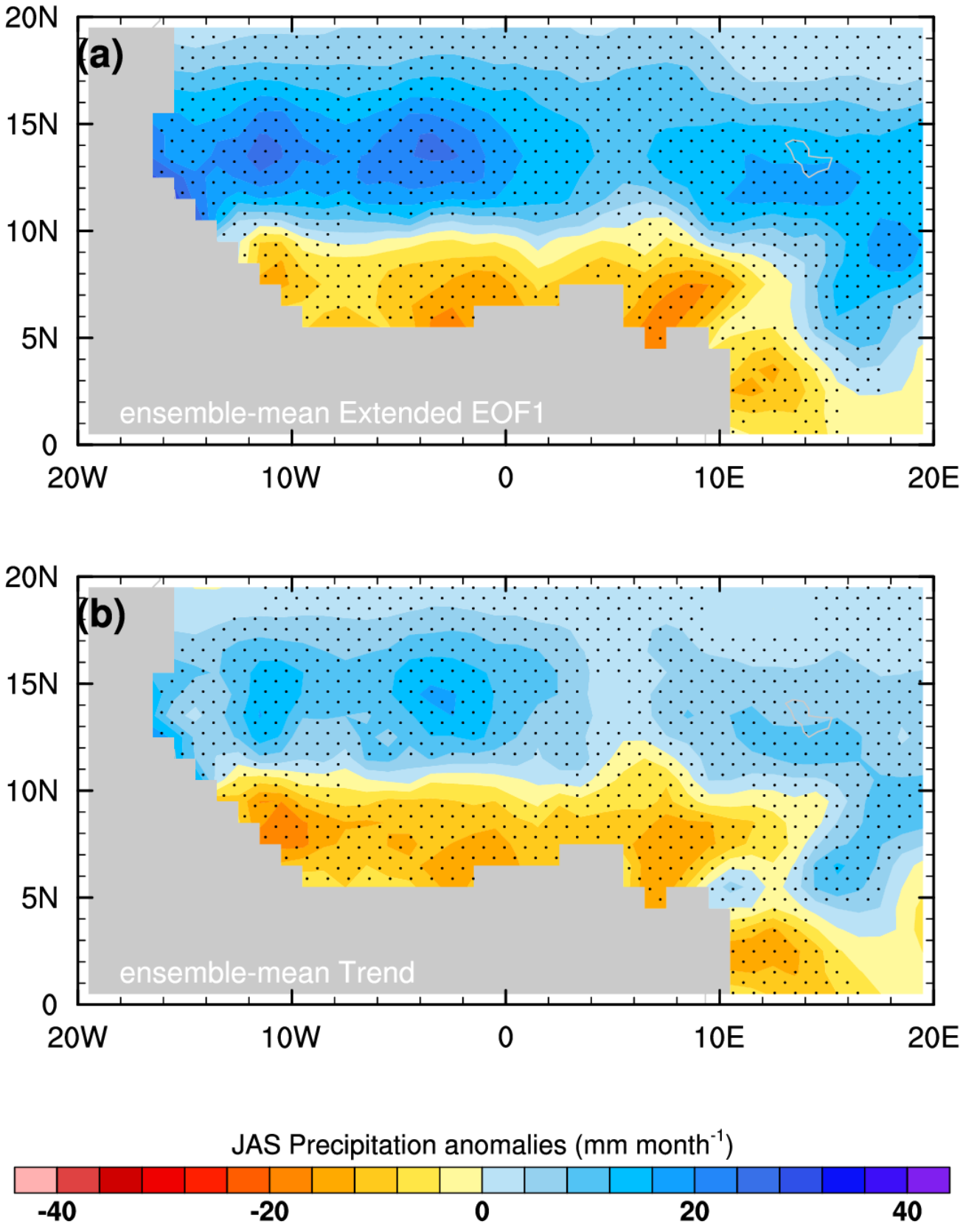

Fig. 6. Multi-data ensemble means of the (a) EOF1 patterns and (b) linear trends of the JAS precipitation over West Africa. The stipples denote statistical significance at the 95% confidence level.

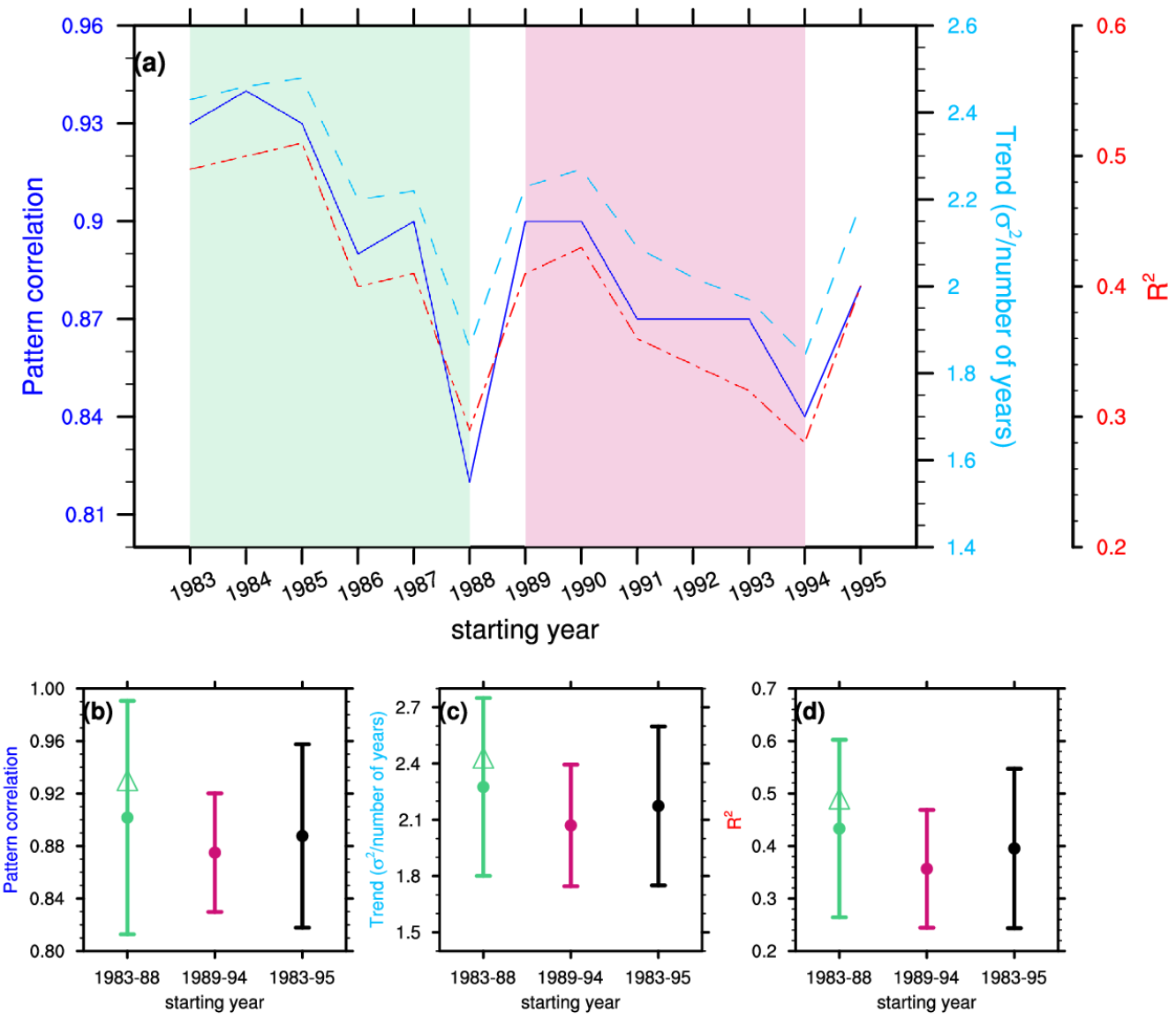

Fig. 7: (a) Left axis: Pattern correlations between the ensemble-mean trend and ensemble-mean extended-EOF1 maps; right axes: the linear trend of PC1 and PC1 variance explained by linear trend using different chunks from 1983-1995 to 2017. Note that the trend estimate has been scaled by the number of years in each chunk which ranges from 23 years (1995-2017) to 35 years (1983-2017). (b) The 95% confidence limit of the pattern correlation, (c) PC1 linear trend and (d) PC1 variance explained by linear trend from 1983-87 (green band in (a)), 1989-93 (pink band in (a)) and 1983-95 to 2017. In b-d, the triangular symbols denote the values for 1983-2017.

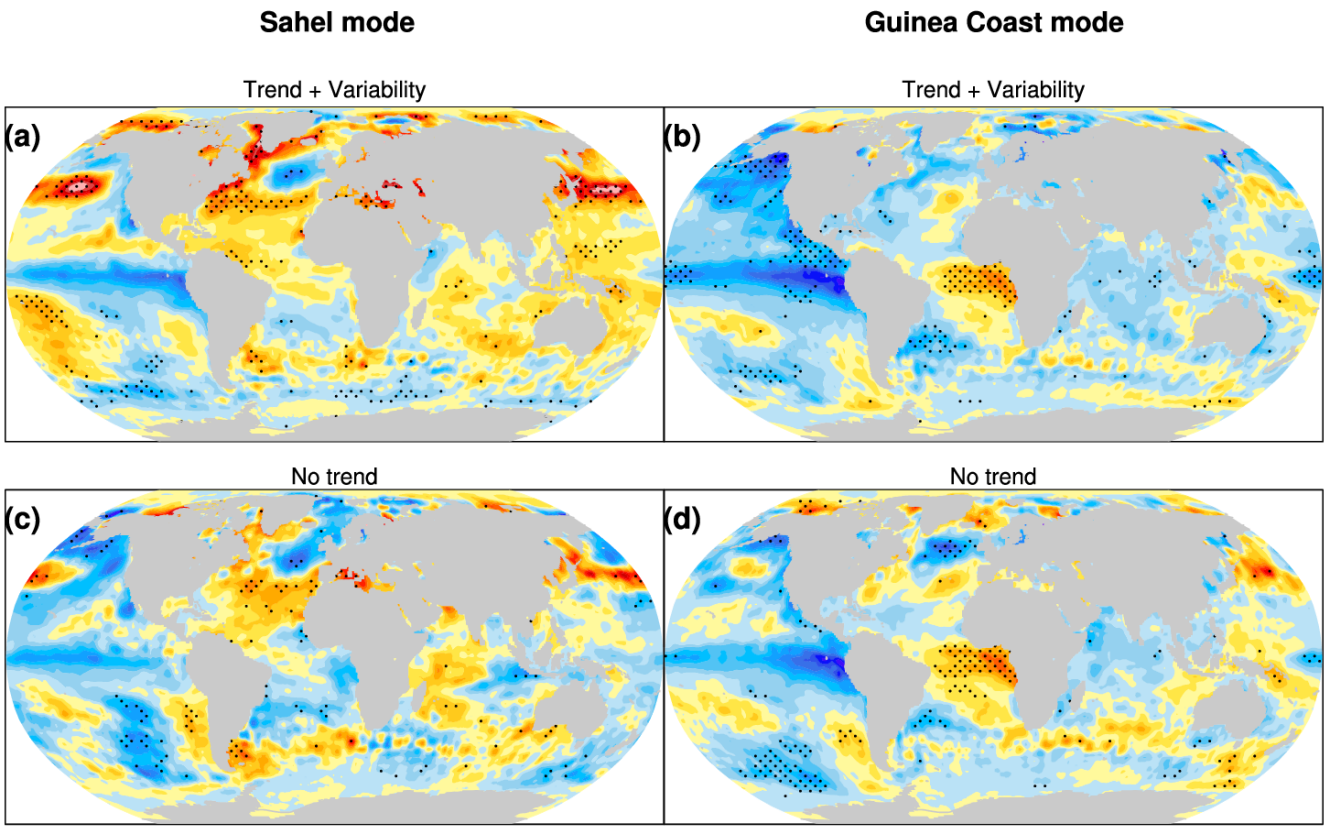

Fig. 8. Composite of the global SST anomalies for the Sahel (a,c) and Guinea Coast modes (b,d) with the raw (a,b) and detrended data (c,d). Stipples denote statistical significance at the 90% confidence level.

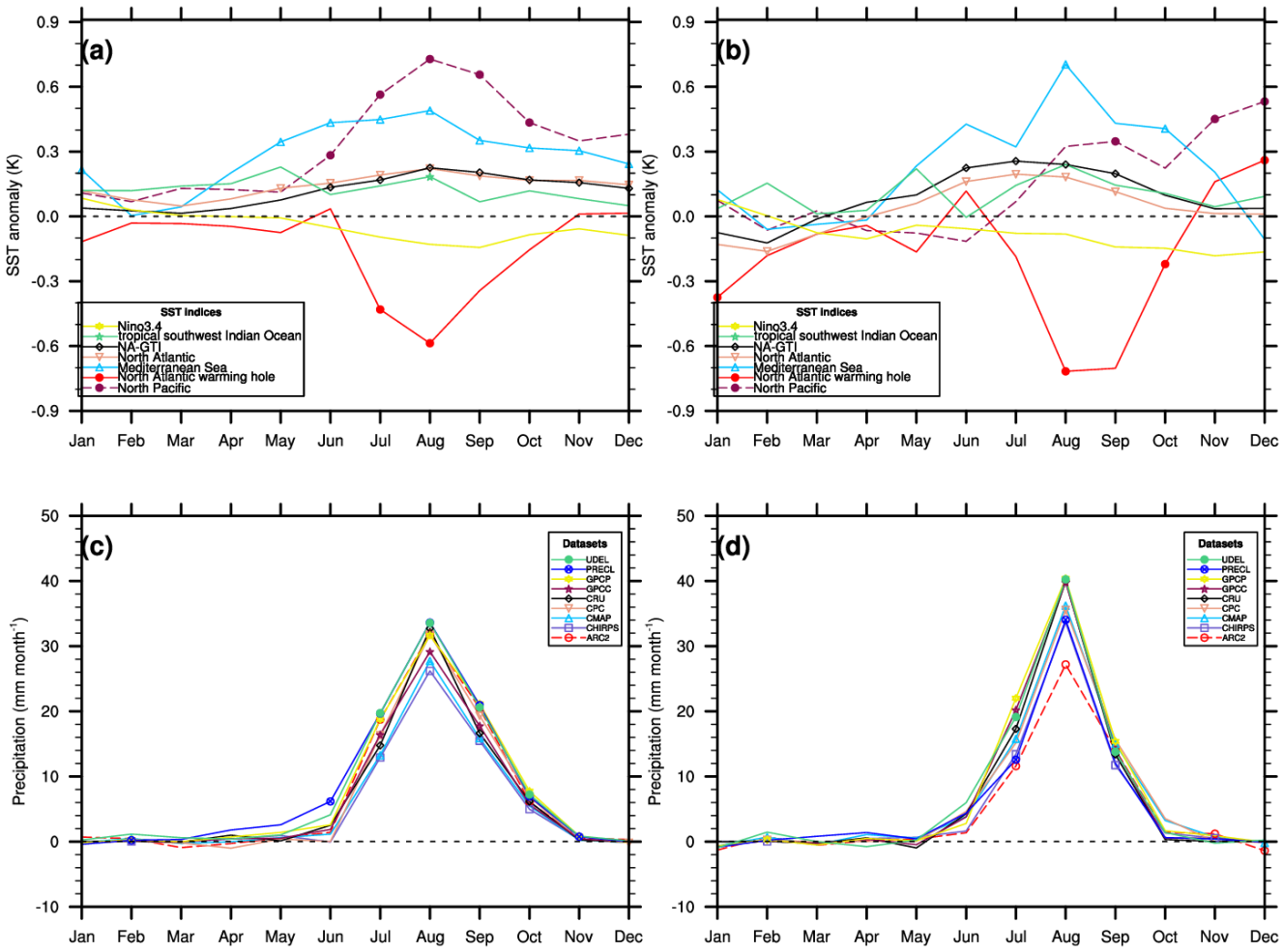

Fig. 9. Composite seasonal evolution of the (a,b) NA-GTI (North Atlantic minus global tropics index), and SST anomalies averaged over the North Atlantic, tropical southwest Indian Ocean, Mediterranean Sea, North Atlantic warming hole, North Pacific and (c,d) the associated Sahel-averaged summer precipitation anomalies. Tick marks denote statistical significance at the 90% confidence level.

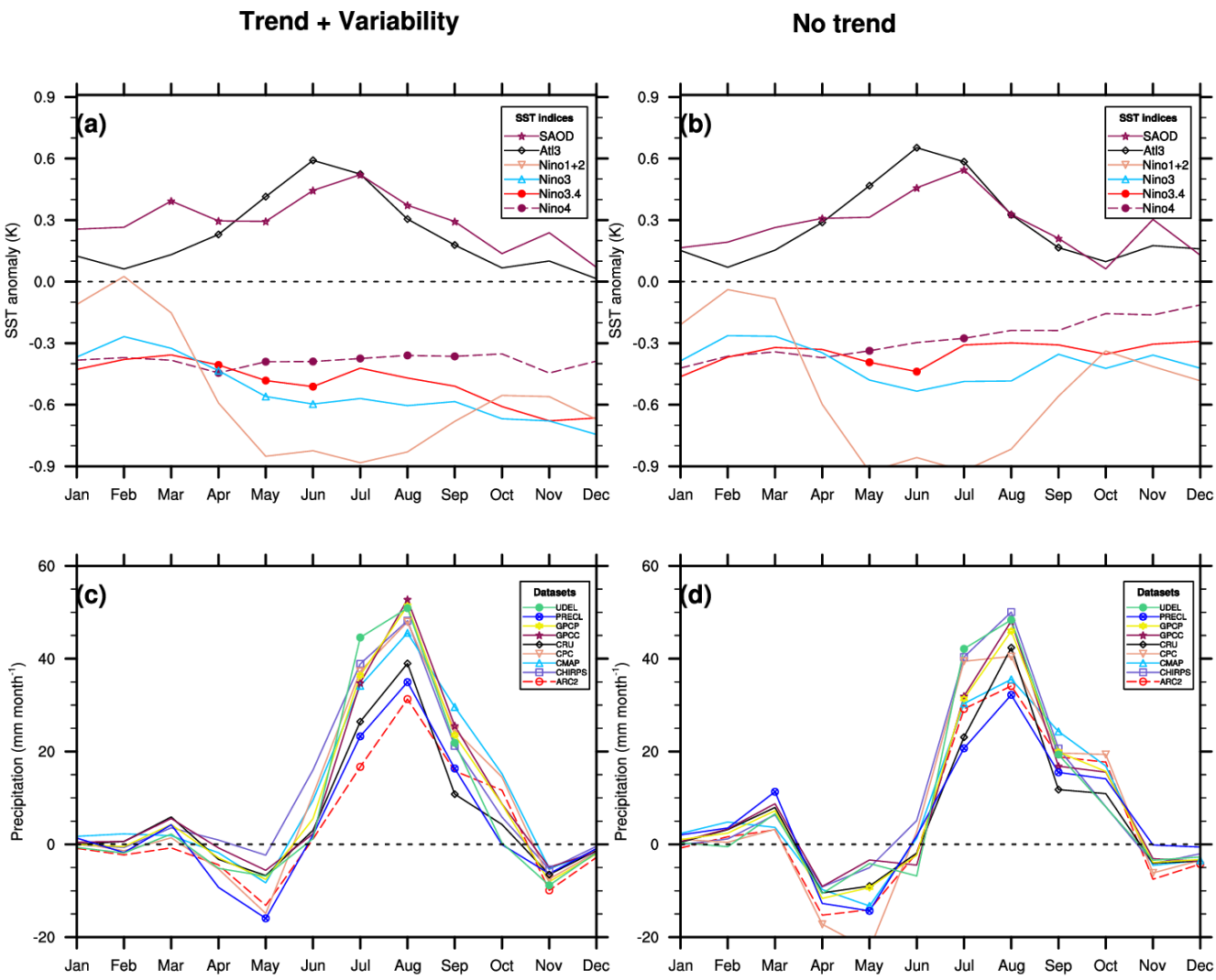

Fig. 10. Composite seasonal evolution of the (a,b) SAOD (South Atlantic Ocean dipole), Atl3, Niño1+2 Niño3, Niño3.4 and Niño4 and (c,d) the associated Guinea Coast summer precipitation anomalies. Tick marks denote statistical significance at the 90% confidence level.

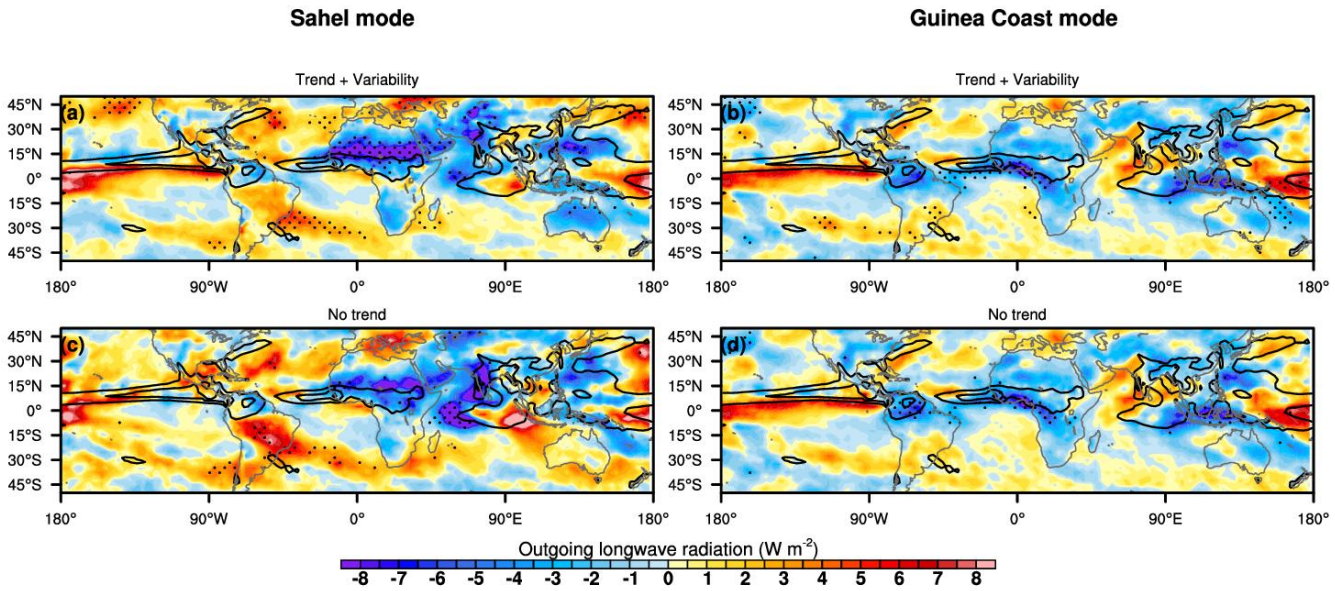

Fig. 11. Composite anomalies of the OLR anomalies for the Sahel (a,c) and Guinea Coast (b,d) modes with the raw (a,b) and detrended data (c,d). Stipples denote statistical significance at the 90% confidence level. Black contours show regions where the mean JAS precipitation is ≥5 mm day^{-1} at an interval of 5 mm day^{-1}.

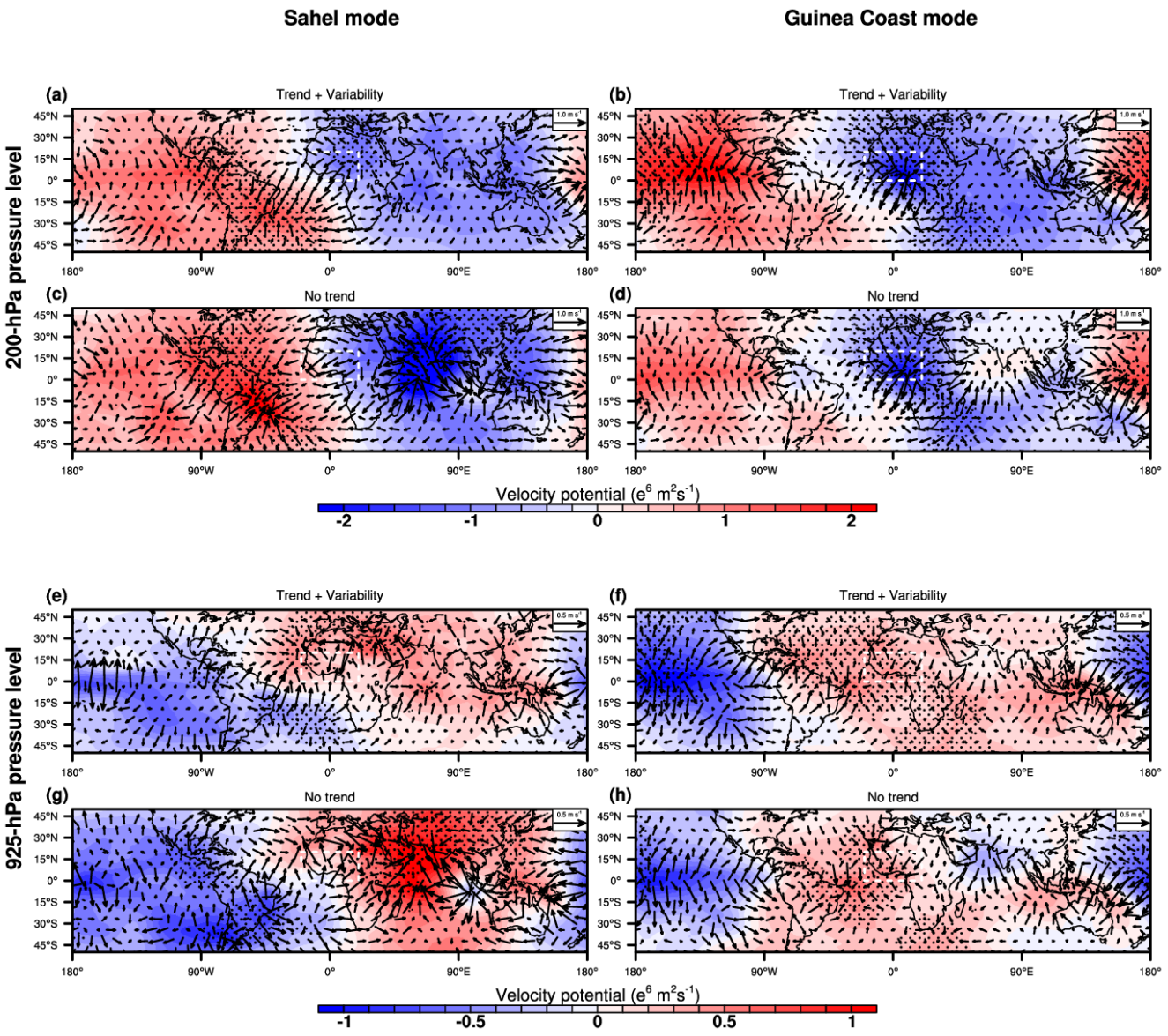

Fig. 12. Composite anomalies of the velocity potential (colour shading) and divergent winds (vectors) at the 200-hPa for the Sahel (a,c) and Guinea Coast (b,d) modes for the raw (a,b) and detrended data (c,d). Stipples denote statistical significance at the 90% confidence level. Panels e-h are similar to but for the 925-hPa level. The rising (sinking) cells of the mean Walker Circulation occur over the continents (oceans).

conflict of interest

Declaration of interests

☐√ The authors declare that they have no known competing financial interests or personal relationships that could have appeared to influence the work reported in this paper.

☐The authors declare the following financial interests/personal relationships which may be considered as potential competing interests:

Leading patterns of the satellite-era summer precipitation over West Africa and global associated teleconnections

Hyacinth C. Nnamchi[a], Victor N. Dike[b,c] and Akintomide A. Akinsanola[d] and Ugochukwu K. Okoro[e]

[a]GEOMAR Helmholtz Centre for Ocean Research Kiel, Düsternbrooker Weg 20, 24105 Kiel, Germany

[b]International Center for Climate and Environment Sciences, Institute of Atmospheric Physics, Chinese Academy of Sciences, Beijing 100029, China

[c]Energy, Climate, and Environment Science Group, Imo State Polytechnic Umuagwo, Ohaji, PMB 1472 Owerri, Imo State, Nigeria

[d]Department of Geography, University of Georgia, Athens, Georgia, United States of America

[e]Atmospheric Physics Group, Department of Physics, Imo State University, Owerri, Nigeria

Author Contributions

H.C.N: Conceptualization, Methodology, Software, Formal Analysis, Visualization, Writing - Original Draft, Writing - Review & Editing.

V.N.D: Methodology, Software, Formal Analysis, Visualization, Writing - Review & Editing.

A.A.A: Methodology, Software, Formal Analysis, Visualization, Writing - Review & Editing.

U.K.O: Methodology, Writing - Review & Editing.